Reviews

ESR and quantum-chemical studies of the structure and thermal transformations of vinylcyclopropane radical cations in irradiated frozen Freon matrices. Simulation of radical processes in the gas phase

*I. Yu. Shchapin,[a] V. I. Fel'dman,[a] V. N. Belevskii,[b] N. A. Donskaya,[b] and N. D. Chuvylkin[c]**

[a]*L. Ya. Karpov Research Physico-Chemical Institute, 10 ul. Obukha, 103064 Moscow, Russian Federation. Fax: +7 (095) 975 2450*
[b]*Department of Chemistry, M. V. Lomonosov Moscow State University, Leninskie Gory, 119899 Moscow, Russian Federation. Fax: +7 (095) 939 0126*
[c]*N. D. Zelinsky Institute of Organic Chemistry, Russian Academy of Sciences, 47 Leninsky prosp., 117913 Moscow, Russian Federation. Fax: +7 (095) 135 5328*

Thermal trasfomations of vinylcyclopropane (VCP) radical cations (RC) in X-ray irradiated frozen Freon matrices, $CFCl_2CF_2Cl$ and $CFCl_3$, were studed by ESR. Radical processes involving $VCP^{\cdot+}$ in very rarefied and moderately thickened gaseous VCP were simulated. Monomolecular cleavage of the cyclopropane ring of *gauche*-$VCP^{\cdot+}$ (**1**) occurs to give the more thermally stable distonic radical cation *dist*(0.90)-$C_5H_8^{\cdot+}$ (**3**). As the density of VCP increases RC **3** adds at the double bond of *anti*-VCP to give the distonic RC, $^{\cdot}CH_2CH_2CHCH(CH_2)_3CHCHCH_2^+$ (**5**). Under the same conditions, the less thermally stable *anti*-$VCP^{\cdot+}$ (**2**) undergoes monomolecular isomerization into RC **1** or reacts with *anti*-VCP with the rearrangement (as in the condensed phase) to give its distonic form, *dist*(90.0)-$C_5H_8^{\cdot+}$ (**4**). The MNDO-UHF method was adapted for quantum-chemical analysis of the constants of isotropic hyperfine coupling with ^1H and ^{13}C nuclei in neutral and charged hydrocabon radicals, since the standard version of this method inadequately reproduces the structural parameters of low-symmetry (C_1, C_S) paramagnetic species. A quantum-chemical analysis of the radiospectroscopic information and of the stereoelectronic control of thermal transformations of conformers of RC **1** and **2** into their structurally nonequivalent distonic forms **3** and **4**, respectively, was carried out.

Key words: radiolysis; Freon matrices; vinylcyclopropane; primary radical cations; distonic radical cations; dimerization; thermal rearrangements; stereoelectronic control; gas phase; quantum-chemical analysis; ESR; MNDO-UHF.

Translated from *Izvestiya Akademii Nauk. Seriya Khimicheskaya,* No. 2, pp. 212—235, February, 1995.
1066-5285/95/4402-0203 $12.50

Introduction

According to a fairly common opinion,[1] the structures and properties of radical cations (RC) derived from hydrocarbons do not depend in the first approximation on the physical state of the material. In view of this statement, it is a common practice in classical radiation chemistry to transfer the regularities established for the transformations of RC in the gas phase by mass spectrometry to processes occurring during the radiolysis of hydrocarbons in condensed media.[1] However, at this time, a great number of direct and indirect experimental indications of the substantial influence of the physical state on the reactivity and the mechanisms of reactions of RC derived from various classes of hydrocarbons are known.[2]

The development of the method of selective stabilization of organic RC in frozen Freon matrices[3] has made possible further investigations of the structures and physicochemical properties of reactive RC with the aid of ESR spectroscopy. However, the direct comparison of the "solid-phase" results with those obtained by mass spectrometry is hampered due to substantial distinctions in the ways RC are generated and registered. Previously it has been suggested[4] that varying the experimental conditions (composition of the matrix, temperature, and concentration) should allow one in principle to simulate the behavior of RC in various physical states using experiments with Freon matrices.

In order to experimentally verify this suggestion, we used frozen Freon solutions of vinylcyclopropane (VCP) irradiated with X-rays and attempted to simulate chemical reactions of the VCP RC in condensed and gas media. The previous communication[4] was devoted to the simulation of the radical transformations of $VCP^{\cdot+}$ in the solid phase. In the present paper we have systematized the procedures and the results of the analogous simulation of gas-phase radical processes involving $VCP^{\cdot+}$.

The procedure for simulation of the gas-phase conditions

The existence of the "gas-phase" medium (the separation of RC) in frozen Freon matrices, γ- or X-irradiated at 77 K, is mostly due to the fact that contact between RC and the original molecules of the dissolved substance is prevented. For this purpose, Freon-11 ($CFCl_3$) is commonly used. At low temperatures this polycrystalline matrix strictly prevents the translational motion of molecules and their RC, but allows the RC to take the most energetically favorable conformation possible through internal rotation and structural rearrangement. The "gas-phase" conditions for the RC occur in this matrix over a wide range of concentrations of the dissolved compound (0.01—1.0 mol. %) and temperatures (77—150 K).

On the other hand, the glass-like matrix of Freon-113 ($CFCl_2CF_2Cl$) is mostly used for simulating ion-molecular reactions in condensed media.[4] However, it is shown below that a very high dilution of solutions (0.01—0.1 mol. %) in a narrow temperature range (77—110 K) makes it possible to also simulate the gas-phase conditions for the RC of the dissolved compound.

The ion-molecular reactions of RC in Freon-113 that occur when the specimens are heated to 110±5 K are due to the restoration of local translational mobility at typical distances (~25 Å). These are the distances that separate the RC from the nearest molecules at a concentration of the dissolved substance of ~1.0 mol. %. At the same time, the macroscopic mobility of the molecules and RC at characteristic distances of more than 100 Å is not restored under these conditions, which is indicated by the fact that even the much more mobile neutral radicals (the products of the ion-molecular reactions) located more than 100 Å apart in the matrix do not interact with each other (do not recombine).

When the concentration of the dissolved compound is very low (0.01 mol. %), the distances between its molecules (in the absence of specific association) are less than 100 Å, *i.e.*, they are not less than those between the neutral radicals in more concentrated solutions. In these cases, local translational mobility cannot ensure the efficient interaction of the RC with the neutral molecules during heating of the sample. Moreover, the concentration of the molecules of the dissolved compound only decreases because of their indirect ionization under irradiation.

In the case of highly dilute solutions, this decrease may be rather pronounced. In fact, a simple estimation shows that at an initial concentration of the additive of 0.01 mol. % and a normal radiation yield G of ~ 0.5 particles per 100 eV at an irradiation dose of 0.5 Mrad, ~50 % of the starting neutral molecules of the admixture undergo indirect ionization.[5] Therefore, the probability of ion-molecular reactions of the RC in highly dilute solutions of the hydrocarbon in Freon-113 is extremely low (at least, for the 77—110 K temperature range). Thus, under these conditions, in addition to the matrix or admixture fluorine- and chlorine-containing radicals, only "separated" (primary or secondary) RC, substantially remote (as in a rarefied gas) from each other and from the original neutral molecules, can be observed.

Thermal transformations of RC in X-irradiated dilute solutions of VCP in Freon-11 or -113 according to ESR data

The ESR spectrum recorded at 150 K of a solution of VCP (0.1 mol. %) in Freon-11, irradiated with X-rays at 77 K, presented in Fig. 1, *a* may be interpreted (Fig. 1, *b*) as a superposition of signals from two types of radicals. The signal with splittings a_1(2 H) = 10.7 Oe,

Table 1. Parameters of the ESR spectra of the $VCP^{\cdot+}$ radical cations and related structures

Radical (N)	Matrix	Temperature /K	g-Factor	The IHFC constants $\lvert a^{H}_{iso}\rvert$ /Oe	References
gauche-$VCP^{\cdot+}$ (**1**)	Freon-113	100	2.0034(4)	13.0 (CH_2=), 7.3 (CH=), 26.0 (1 H)	4
	Freon-11	150	2.0034(4)	10.7 (CH_2=), 6.4 (CH=), 26.8 (1 H)	*
anti-$VCP^{\cdot+}$ (**2**)	Freon-113	100	2.0034(4)	13.0 (CH_2=), 7.3 (CH=), 2.7 (1 H)	4
dist(0.90)-$C_5H_8^{\cdot+}$ (**3**)	Freon-113	110	2.0034(4)	21.6 (2 H(α)), 14.7 (2 H(β))	*
dist(90.0)-$C_5H_8^{\cdot+}$ (**4**)	Freon-113	113	2.0034(4)	22.7 (2 H(α)), 30.4 (2 H(β))	4
$\cdot CH_2CH_2CHCH(CH_2)_3CHCHCH_2^+$ (**5**)	Freon-113	113	2.0034(4)	22.7 (2 H(α)), 30.4 (2 H(β))	*
$\cdot CH_2CH_2CH{=}CH_2$ (**6**)	Cyclopropane	168	—	22.2 (2 H(α)), 28.5 (2 H(β))	12
$(CH_3)_2C\cdot CH_2C^+HCH_3$ (**7**)	Freon-113	115	2.0029	23.6 (2 CH_3), 11.8 (2 H(β))	6
$(CH_3)_2C\cdot CH_2C^+(CH_3)$ (**8**)	Freon-113	117	2.0029	23.3 (2 CH_3), 11.7 (2 H(β))	6

* This work.

a_2(1 H) = 6.4 Oe, and a_3(1 H) = 26.8 Oe (Fig. 1, *c*; Table 1) corresponds to *gauche*-$VCP^{\cdot+}$ **(1)**,[4] and the other signal is associated with *anti*-$VCP^{\cdot+}$ **(2)** (Fig. 1, *d*, Scheme 1).

Since none of the lines for *anti*-$VCP^{\cdot+}$ is exhibited individually in the ESR spectrum (Fig. 1, *a*), the splittings previously evaluated for *anti*-$VCP^{\cdot+}$ in Freon-113 [4] were used in the simulation of the spectrum. The simulated spectrum for equal proportions of *gauche*- and *anti*-$VCP^{\cdot+}$ (Fig. 1, *b*) is identical to that of a dilute solution of VCP (0.1 mol. %) in Freon-11 irradiated at 150 K (Fig. 1, *a*). Varying the ratio between *gauche*- and *anti*-$VCP^{\cdot+}$ allows one to represent all of the characteristic features of the ESR spectra of irradiated solutions of VCP in Freon-11 over the whole ranges of both concentrations (0.01—20.0 mol. %) and temperatures (77—150 K) studied.

Scheme 1

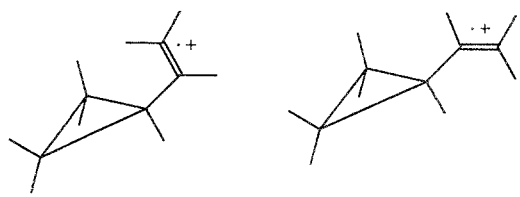

1 **2**

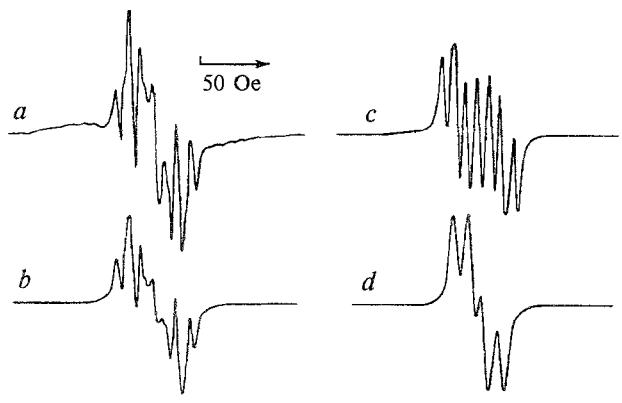

Fig. 1. The ESR spectrum of a solution of VCP in $CFCl_3$ (0.1 mol. %), X-irradiated (0.5 Mrad) at 77 K, recorded at 150 K (*a*). Simulated spectra: a mixture (1:1) of *gauche*-$VCP^{\cdot+}$ and *anti*-$VCP^{\cdot+}$ (*b*); *gauche*-$VCP^{\cdot+}$, a_1(2 H) = 10.7 Oe, a_2(1 H) = 6.4 Oe, a_3(1 H) = 26.8 Oe, the line width ΔH = 5.0 Oe with Lorentzian contribution L = 0.2 (*c*); *anti*-$VCP^{\cdot+}$, a_1(2 H) = 13.0 Oe, a_2(1 H) = 7.3 Oe, a_3(1) = 2.7 Oe, the line width ΔH = 6.0 Oe with Lorentzian contribution L = 0.2 (*d*).

In Freon-11, the constants of isotropic hyperfine coupling (IHFC) with the protons of the vinyl group of *gauche*-$VCP^{\cdot+}$ are 15 % lower than those in Freon-113 (see Table 1). This effect of the matrix is well known and is due either to a partial transfer of the unpaired electron to the $CFCl_3$ molecule, which forms a strong complex with the RC,[6,7] or to the twisting of the vinyl fragment due to the ionization of the double bond.[8] The former explanation is preferable, since the simultaneous decrease in the IHFC constants for the hydrocarbon RC and increase in their stability in Freon-11 occur whether or not there are ionized double bonds in them.[7]

The ratio between the *gauche* and *anti* isomers of $VCP^{\cdot+}$ also depends significantly on the matrix type. In the "diffusionally soft" Freon-113, the proportion of *gauche*-$VCP^{\cdot+}$ was only 0.04,[4] whereas in the "diffusionally rigid" Freon-11, it is close to 0.5, *i.e.*, it is even higher than the proportion of *gauche*-VCP molecules (0.25) in the gas phase.[9] As cooling of solutions of VCP in Freons (to 77—150 K) can only result in a decrease in the content of the less stable conformer, *gauche*-VCP,[9] the increase in its content to 0.5 as a result of ionization reflects the fact that a substantial portion of the ionized *anti*-VCP molecules are transformed to the *gauche*-$VCP^{\cdot+}$ conformation, which is more favorable under the "gas-phase" conditions.

$$\underset{\mathbf{2}}{\textit{anti}\text{-}VCP^{\cdot+}} \rightarrow \underset{\mathbf{1}}{\textit{gauche}\text{-}VCP^{\cdot+}} \qquad (1)$$

The preference for the *anti* or *gauche* conformation depends on the positive charge, Q^{VCP}, localized at the VCP fragment. When Q^{VCP} is 0.0 to 0.5 (as in the molecule of *anti*-VCP or the π-[*anti*-$VCP]_2^{\cdot+}$ RC, respectively), the *anti*-conformation is more stable,[4,9] and when $Q^{VCP} \approx 1.0$ (as in the *gauche*-$VCP^{\cdot+}$ RC) the *gauche* form is more stable.

The ESR spectrum of a highly dilute (0.01 mol. %) solution of VCP in Freon-113, X-irradiated at 77 K, (Fig. 2, *a*) exhibits a poorly resolved, very extended (250—300 Oe) anisotropic ESR signal, wherein the *g* factor is greater than that for the free electron (2.0023) and hydrocarbon RC. As the temperature is increased to 100 K, this signal reversibly disappears and no longer hampers the study of the ESR spectra of the radicals derived from the admixture introduced in Freon-113 (0.01 mol. %). The poorly resolved signal is probably associated with the matrix radicals.

The ESR spectrum recorded at 110 K (see Fig. 2, *b*) is a well-resolved triplet of triplets with the binomial ratio between the intensities of the lines and the splittings, $a_1(2\ H) = 21.6$ Oe and $a_2(2\ H) = 14.7$ Oe, characteristic of *n*-alkyl radicals of the type $\cdot CH_2CH_2Z$ in which two equivalent C—H bonds form dihedral angles of $\theta_1 = \theta_2 = 60°$ with the axis of the unpaired electron p-AO. This well-resolved spectrum is only recorded in a narrow temperature range of 100—110 K.

The spectrum (see Fig. 2, *b*) of the $\cdot CH_2CH_2Z$ radical with the dihedral angles $\theta_1 = \theta_2 = 60°$ is substantially different from the ESR signals of *anti*- and *gauche*-$VCP^{\cdot+}$. Under the conditions used (see above) this specific radical could only result from a monomolecular transformation of the primary $VCP^{\cdot+}$ and, hence, it is also an RC. Judging by the IHFC constants (see Table 1), this RC has the conformation of *dist*(0.90)-$C_5H_8^{\cdot+}$ (**3**), and $Z = CHCHCH_2^+$ (see Ref. 4).

In extremely dilute Freon solutions (*i.e.*, where only the ESR spectrum of the matrix radicals is recorded), the RC additives exist under conditions similar to those in the gas phase. Therefore, only the primary monomeric *gauche*-$VCP^{\cdot+}$ can act as the precursor of the secondary RC, *dist*(0.90)-$C_5H_8^{\cdot+}$. Thus, in the X-irradiated frozen Freon-113 matrix, in the case of an extremely dilute (0.01 mol. %) solution of VCP at 77—100 K, monomolecular cleavage of the cyclopropane ring of the *gauche*-$VCP^{\cdot+}$ **(1)** occurs to give the distonic RC, *dist*(0.90)-$C_5H_8^{\cdot+}$ **(3)**, (Scheme 2, reaction (2)).

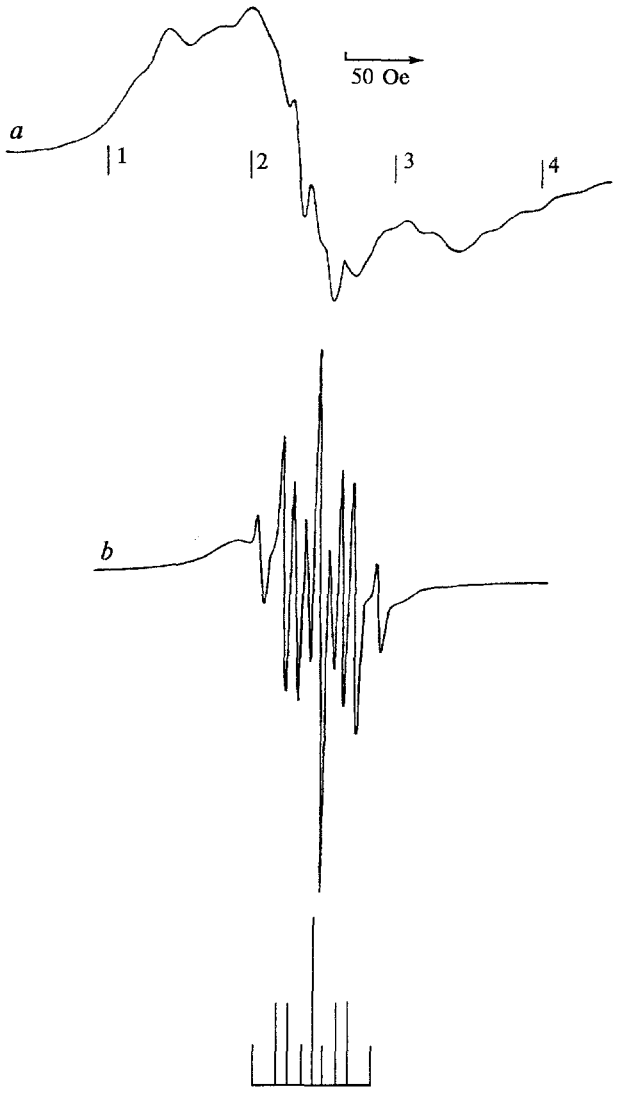

Fig. 2. The ESR spectrum of a 0.01 mol. % solution of VCP in $CFCl_2CF_2Cl$, X-irradiated (0.5 Mrad) and recorded at 77 K (*a*), at 110 K (*b*). The vertical lines 1—4 denote the positions of the corresponding Mn^{2+} lines in MgO.

The ESR spectrum of a dilute (0.1 mol. %) solution of VCP in Freon-113, X-irradiated at 77 K and recorded at 77 K (Fig. 3, *a*) is a mixture of an unidentified narrow anisotropic signal (whose *g*-factor is greater than that of the free electron) and a singlet associated with $VCP^{\cdot+}$. For comparison, the singlet ESR spectrum corresponding to a more concentrated (0.9 mol. %)

Scheme 2

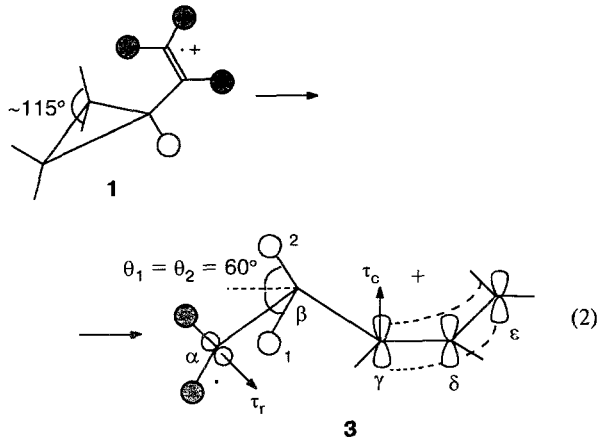

solution of VCP in Freon-113 at 77 K is shown in Fig. 3, *a* by the dashed line.

As the temperature of the sample (0.1 mol. %) is increased to 110 K, this singlet irreversibly disappears, and two triplets of triplets (Fig. 3, *b*) with splittings typical of the $\cdot CH_2CH_2Z$ radical with the dihedral angles $\theta_1 = \theta_2 = 60°$ (see Scheme 2) and $\theta'_1 = \theta'_2 = 30°$ (Scheme 3) appear instead. The noncoincident lines (*1*, *2*) corresponding to these RC **3** and RC **4+5** are marked in Fig. 3, *b*—*d*. These lines make equal contributions to the total integral intensities of the signals for each type of radicals. In the low-field region of the spectrum, the forms of the above-mentioned similar lines are distorted by a foreign anisotropic signal. Therefore, it is convenient to evaluate the proportions of the two above-mentioned radical forms in the sample (0.1 mol. %) using the intensities of the non-distorted lines marked in the high-field region of the spectra. At 110 K, the ratio between the intensities of these lines (see Fig. 3, *b*—*d*, *1* and *2*) is 1:1, while at 113 K it is close to 1:5 and at 121 K it again is 1:1.

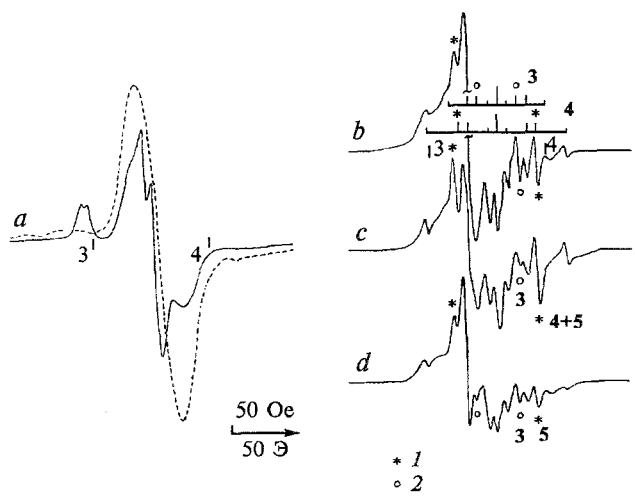

Fig. 3. The ESR spectrum of a 0.1 mol. % solution of VCP in $CFCl_2CF_2Cl$, X-irradiated (0.5 Mrad) and recorded at 77 K (the dashed line corresponds to the similar (77 K) ESR spectrum of a solution of VCP (0.9 mol. %) in $CFCl_2CF_2Cl$) (*a*); 110 K (*b*); 113 K (*c*); 121 K (*d*). The vertical lines 3 and 4 are the positions of the corresponding Mn^{2+} lines in MgO. *1* — RC **3**, *2* — RC **4** and **5**.

Scheme 3

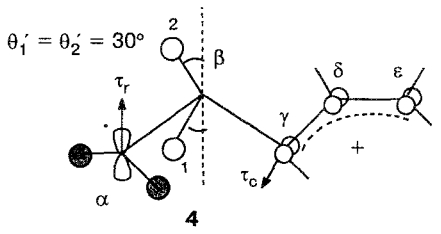

Previously[4] the above-described triplets of triplets with the characteristic splittings (see Fig. 3, *b*) recorded under similar conditions (110 K, Freon-113) were assigned to distonic radical cations, namely, to the monomeric *dist*(0.90)-$C_5H_8^{\cdot +}$ **3** in an extremely dilute solution (0.01 mol. %, Scheme 2) or to the coordinate-bonded *dist*(0.90)-$C_5H_8^{\cdot +}$ (**4**) (see Scheme 3) in the π-dimeric complex [*dist*(90.0)-$C_5H_8^{\cdot +}$...*anti*-VCP] (**4a**) in a concentrated (1.0 mol. %) solution of VCP. In both cases, the proportion of the distonic form of $C_5H_8^{\cdot +}$ is close to 100 %. Thus, at 110 K a dilute (0.1 mol. %) solution of VCP in Freon-113 (see Fig. 3, *b*) contains equal amounts of *dist*(0.90)- and *dist*(90.0)-$C_5H_8^{\cdot +}$ distonic RC. For the reasons discussed below, to account for the changes occurring in the ESR spectra of an 0.1 mol. % sample as the temperature is increased from 110 to 113 K and then to 121 K (Fig. 3, *b*—*d*), one should assume that at 113 and 121 K, in addition to *dist*(90.0)-$C_5H_8^{\cdot +}$ **4**, the sample contains one more distonic RC **5**, which is characterized by a triplet of triplets with the same splittings (see Table 1). At 123 K, the signals for all of the distonic RC irreversibly disappear, and the ESR spectra become poorly resolved and not informative.

Two approaches to the explanation of the above-presented data are possible (Scheme 4). In our opinion, the explanation that postulates **3a** ⇄ **4a** reversible conformational transitions is more controversial, since, when the temperature of the sample increases from 110 to 113 K, all of the subsequent transformations of RC **3** are due to its dimerization with starting VCP molecules. However, it is unclear, how the interaction of the secondary monomeric RC **3** with an *anti*-VCP molecule can result in the formation of RC **4** incorporated in the [*dist*(90.0)-$C_5H_8^{\cdot +}$...*anti*-VCP] **4a** (see Ref. 4) π-dimeric complex.

In fact, the first step of the two-step process (Scheme 5, reactions (5)—(6)), which consists of the successive rotation of the $CHCHCH_2^+$ and $CH_2^{\cdot}$ termi-

Scheme 4

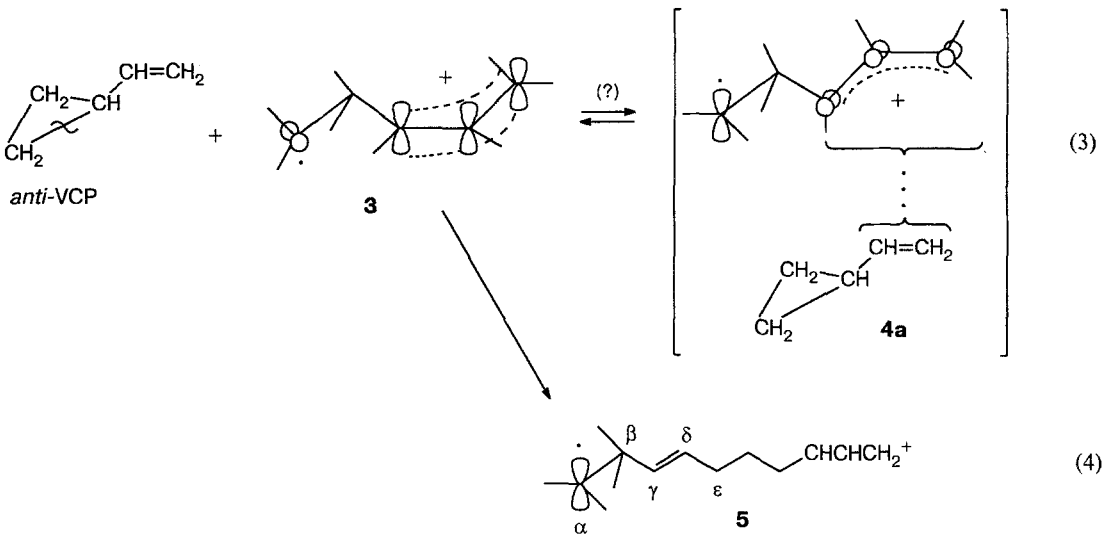

Scheme 5

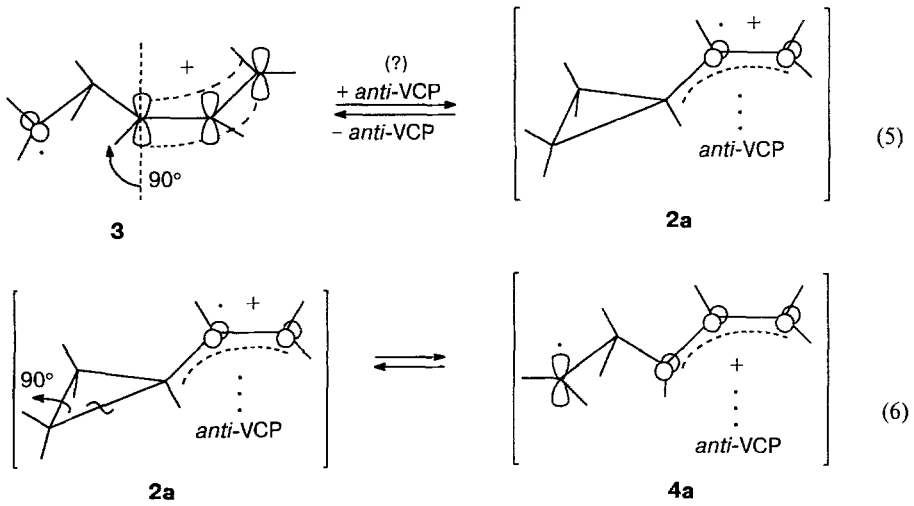

nal groups of the C(α)—C(β)—C(γ) "trimethylene-cyclopropane" fragment in the $C_5H_8^{\cdot+}$ RC through 90°, looks fairly unconvincing. Dimerization of the primary RC, anti-VCP$^{\cdot+}$ **2**, with an *anti*-VCP molecule is known[4] to result in opening of the cyclopropane ring (reaction (6)). Therefore, the reasons why a similar interaction of the *anti*-VCP molecule with monomeric RC **3** (*dist*(0.90)-$C_5H_8^{\cdot+}$) would favor the reverse process, *viz.*, the closure of the cyclopropane ring to yield dimeric complex **2a** (reaction (5)), remain obscure.

On the other hand, in the case of synchronous rotation of the $CHCHCH_2^+$ and $CH_2^{\cdot}$ terminal groups of the C(α)—C(β)—C(γ) "trimethylene-cyclopropane" fragment in the $C_5H_8^{\cdot+}$ distonic RC (see Schemes 2 and 3), it should be expected[10] that 1,2-shifts of the H atoms would result in linear diene radical cations. However, in the case of VCP, we detected no isomeric linear diene RC exhibiting characteristic ESR[11] signals.

An alternative approach (see Scheme 4, reaction (4)) is that the reaction of the secondary monomeric RC **3** (*dist*(0.90)-$C_5H_8^{\cdot+}$) with the *anti*-VCP molecule be considered addition to the terminal methylene group at the double bond of *anti*-VCP to yield distonic RC **5** containing a homoallylic radical site. The conformations and the IHFC constants with the protons of the unsubstituted homoallylic radical, $CH_2{=}CH{-}CH_2{-}CH_2^{\cdot}$ (see Table 1), and of RC **4** (*dist*(90.0)-$C_5H_8^{\cdot+}$) are practically identical.[4,12] Therefore, RC **5** and **4** are indistinguishable by their ESR spectra. Taking this into account (see reactions (1), (2), (4), and (6) in the Schemes) one can easily and consistently explain the above-described changes of the ESR spectra occurring as the concentration and the temperature of the sample vary.

At 110 K, an X-irradiated (0.1 mol. %) solution of VCP in Freon-113 contains equal amounts of mono-

meric RC **3** (*dist*(0.90)-$C_5H_8^{\cdot+}$) and π-dimeric complexes [*dist*(90.0)-$C_5H_8^{\cdot+}$...*anti*-VCP]. When the sample is heated to 113 K, the *dist*(0.90)-$C_5H_8^{\cdot+}$ RC decay according to reaction (4), and the concentrations of RC **5** and **4a** become identical. A further increase in the temperature to 121 K causes destruction of the specific solvation of RC **4** (*dist*(90.0)-$C_5H_8^{\cdot+}$) with the *anti*-VCP molecules, *i.e.*, decomposition of the [*dist*(90.0)-$C_5H_8^{\cdot+}$...*anti*-VCP] π-dimeric complexes.

The structure of **4a** is not very stable, and as the cyclopropane ring is closed, it is converted (reaction (6)) into form **2a**,[4] which is more stable in the condensed medium. The latter eliminates the *anti*-VCP molecule to give the monomeric RC, *anti*-$VCP^{\cdot+}$, which then undergoes a conformational transition (1), because of the higher stability of the monomeric RC, *gauche*-$VCP^{\cdot+}$ under the gas-phase conditions. In turn, *gauche*-$VCP^{\cdot+}$ **1** undergoes opening of the cyclopropane ring (reaction (2)) to give RC **3** (*dist*(0.90)-$C_5H_8^{\cdot+}$). When the concentration of VCP in Freon-113 decreases from 0.1 to 0.01 mol. %, only monomolecular process (2) is detected by ESR, and when the concentration increases from 0.1 mol. % to 1.0 mol. %, thermodynamic equilibrium (6) is observed.

The admixture of *gauche*-$VCP^{\cdot+}$ RC in a solution of VCP (1.0 mol. %) in Freon-113 (see Fig. 2) is characterized by narrower ESR lines and higher values for the a^{H}_{iso} constants of the vinyl group compared with those for a solution in Freon-11 (Fig. 1, *a*). This means that in the Freon-113 matrix, the admixture radical cations, *gauche*-$VCP^{\cdot+}$, exist under conditions that are rather close to gas-phase conditions, since they are not only actually separated from each other (as in Freon-11), but also experience no radiospectroscopically detectable effect of the matrix. Hence it follows that the occurrence of selective irreversible isomerization (2) in highly dilute (0.1—0.01 mol. %) solutions of VCP in Freon-113 indicates that the cyclic monomer, *gauche*-$VCP^{\cdot+}$ **1**, is less thermodynamically stable in the gas phase than the distonic conformer, *dist*(0.90)-$C_5H_8^{\cdot+}$ **3**.

In a concentrated (1.0 mol. %) solution of VCP in Freon-113, primary *gauche*-$VCP^{\cdot+}$ **1** at 100 K and secondary *dist*(0.90)-$C_5H_8^{\cdot+}$ **3** at 113 K are observed as admixtures (several hundredths) to RC **2a** and **4a**, which predominate in the condensed phase.[4] Therefore, even in this solution, some of the RC existing under the gas-like conditions are involved in gas-phase isomerization (2), rather than in thermodynamic equilibrium **2a** ⇌ **4a** (equation (6)). In other words, at 77—113 K in Freon-113, in addition to the stabilized forms of $VCP^{\cdot+}$ inherent in the solid phase, analogous RC exist independently in structurally separated areas that simulate the gas phase. According to the data of Figs. 2, *b* and 3, *b* and Refs. 4 and 13, the number of these areas is independent of the concentration of the additive. Therefore, as the solution of VCP in Freon-113 is diluted from 1.0 to 0.01 mol. %, their contribution becomes predominant, while the proportion of the "solid-phase" regions of the stabilization of $VCP^{\cdot+}$ decreases by a factor of 100.

Quantum-chemical analysis of the ESR spectra and thermal transformations of the hydrocarbon RC

Many research centers study the structures and reactivities of hydrocarbon RC.[2—4,14—19] The combination of quantum-chemical calculations with the "convenient" version of ESR (separation of RC in inert or Freon matrices) has been the most informative method of analysis.[4,15] Recently, first communications concerned with the determination of the geometry of RC using quantum-chemical calculations combined with IR-spectroscopy data have been published.[20,21] Previously Gleiter[22] attempted to obtain structural and chemical information on hydrocarbon RC from their photoelectron spectra.

Trustworthy quantum-chemical calculations of the magnetic properties of RC are particularly significant for the reliable identification of ESR spectra when their intuitive structural interpretations are ambiguous. This applies, in particular, to hydrocarbon RC with nearly degenerate boundary MO, since in this case, along with the specific spin-orbital effects, the influence of the medium on the resonance parameters should also be taken into account.[23—26] On the other hand, the mixed ESR spectra of $VCP^{\cdot+}$, presented previously[4] and in the present work, are difficult to interpret, due to the superposition of the poorly resolved signals from the isomeric radical forms such that one of these forms (*anti*-$VCP^{\cdot+}$) is not individually manifested in the spectra. In these cases, the spectral characteristics are usually estimated either semi-intuitively (based on accumulated experience), or using specialized calculation programs meant for the computer simulation of complex ESR spectra.[27] The interpretation of these spectra can be considerably simplified by invoking adequate nonempirical or semiempirical quantum-chemical methods.

The theoretically determined magnetic-resonance parameters of free radicals are known[28,29] to be very sensitive to inaccurate choices for their geometry. Meanwhile, information on the structures of any free radicals is scanty, and for the hydrocarbon RC, this information is, moreover, quite controversial.[6,8,10,30—37] Therefore, in solving the problem of the geometric parameters of complex RC, one is often forced either to rely again on intuition[25,38] or to use the assumptions of simplified quantum-chemical methods, the accuracy of which dramatically decrease, as a rule, as the symmetries of the radicals decrease.[28]

In fact, there is strong evidence that the geometric structures of the ground states of low-symmetry (C_1, C_2, C_S) neutral and charged radicals are represented with great errors not only in terms of common semiempirical self-consistent schemes like INDO and MNDO,[28] but also in terms of modern "refined" nonempirical methods

with rather extensive basis sets, like 6-31 G**, and efficient consideration of the electron correlation.[8,32] In turn, these errors in the structural parameters cause substantial discrepancies between the simulated and experimental ESR spectra.[8,28,32]

Only in some instances can satisfactory agreement be achieved between the nonempirically calculated (MP2/6-31 G**) and the experimentally measured IHFC constants for hydrocarbon RC, and, based on this, can the preliminarily optimized geometric parameters of the RC be given the status of "certain".[28] In these cases, the effect of the matrix environment on the magnetic-resonance characteristics of the RC was assumed to be negligibly small.[31] At the same time, a doubtful practice appeared[10] to explain the substantial discrepancies between the theoretical and experimental results by the effect of the matrix, despite convincing examples of the inadequacy of the quantum-chemical methods used.[8,30] The semiempirical[39–44] and nonempirical[10,32,35,36,39,44–48] calculations of the potential energy surfaces describing rearrangements of hydrocarbon RC *via* transition states having no symmetry elements should be examined much more carefully, since the results of these calculations[8,30,33] are often at variance with experimental data[8,30,33,49] even for the original low-symmetry ground states of the RC.

On the other hand, it has been shown previously[28] that the unsatisfactory correlation found[50] between MNDO-calculated and experimental IHFC constants, a^{Z}_{iso}, where Z = ^{1}H, ^{13}C, ^{14}N, ^{17}O, is due most of all to the great deviations of the structural parameters of the radicals from the reliable values, which is typical of low-symmetry radicals. For the systematic quantum-chemical calculations of the magnetic-resonance parameters using the reliable geometry of free radicals, in addition to the INDO-UHF approximation, the intrinsically noncontradictory MNDO-UHF version was suggested.[28] In this method, the transition from the calculated spin densities (ρ_s^H) to the IHFC constants with protons ($a^{H}_{iso} = K(H)\rho_s^H$) is accomplished using two proportionality coefficients ($K(H(\alpha)) = 508$ Oe for $\rho_s^H < 0$ and $K(H(\beta)) = 850$ Oe for $\rho_s^H > 0$).

Taking the foregoing into account, we systematized the particular suggestions on the adequate selection of the structural parameters of hydrocarbon RC necessary for the reliable calculation of the a^{H}_{iso} IHFC constants (Z = ^{1}H, ^{13}C) by the MNDO-UHF method. Moreover, we specially adjusted the $K(H(\alpha))$ and $K(H(\beta))$ coefficients of proportionality for the hydrocarbon free radicals, since, as follows from the published data,[28] they depend on the type of atom bearing the proton. Using the adapted MNDO-UHF method (below referred to as AMNDO-UHF), we calculated the a^{H}_{iso} constants for the VCP$^{\cdot+}$ radical cation and carried out the quantum-chemical analysis of the electronic and geometric factors determining the formation, stabilization, and low-symmetry thermal transformations of primary radical forms into distonic structures.

Testing the standard MNDO-UHF method

In order to verify the efficiency of using the standard MNDO-UHF scheme to investigate the spin distribution in hydrocarbon radical systems, we carefully selected a series of neutral and charged radicals (Table 2) that had been characterized by both reliable experimental IHFC constants and certain structural parameters obtained by spectroscopic measurements and *ab initio* calculations in an extended basis set of the 6-31 G* type taking into account the electron correlation. For each of these radicals, the spin density distribution with the fixed certain geometry (I) was calculated in terms of the standard MNDO-UHF method followed by the calculation for the geometry (II) fully optimized by the MNDO-UHF method.

All of the calculations were carried out using the MNDO quantum-chemical program.[51] The correlations of the calculated spin densities with the experimental a^{Z}_{iso} IHFC constants were performed according to the standard procedure:[50]

$$a^{Z}_{iso} = K(Z)\rho_s^{Zn}, \qquad (1^*)$$

where $K(Z)$ is the proportionality coefficient for each type of atom Z, and ρ_s^{Zn} is the spin population of the valence s-atomic orbital (AO) of the particular Z_n atom. The correlation coefficients (r^Z) between the theoretical and experimental a^{Z}_{iso} IHFC constants were determined by the standard method.[52]

Table 2 presents the reliable (I) and MNDO-UHF fully optimized (II) structural parameters for the neutral and charged radicals **9**—**16**. Specifications of the atoms in some of them are given in Scheme 6. For C_2H_3 (**12**), the geometry optimized in the STO-3G basis was taken as certain, since this or rather close geometry was used in all of the known nonempirical calculations of the IHFC constants.[29,52] The experimental IHFC constants with the ^{1}H and ^{13}C nuclei for radicals **9**—**16** are given in Table 3, along with those calculated *ab initio* and in terms of the two semiempirical schemes being compared.

Scheme 6

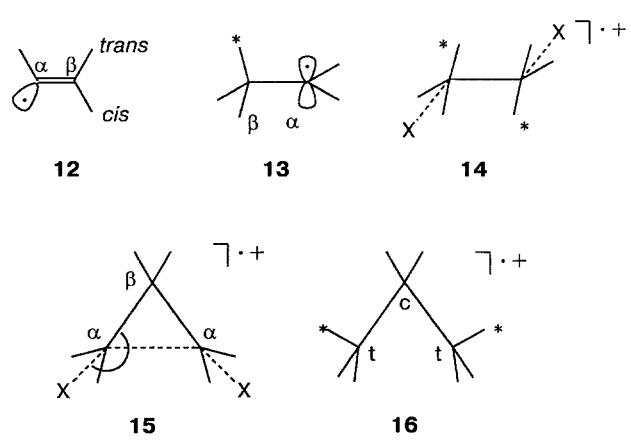

Table 2. The geometric parameters (XY bond lengths, Å and XYZ bond angles, deg) for neutral and charged hydrocarbon radicals

Radical	Symmetry (ref.)	Geometric parameter	Type of geometry I (*ab initio*)	Type of geometry II (MNDO)	Δ
$CH_2^{\cdot -}$	C_{2v}[a]	C—H	1.121	1.107	−0.014
9	(53)	HCH	104.4	107.0	2.6
CH_3	D_{3h}[a]	C—H	1.079	1.078	−0.001
10	(54)	HCH	120.0	120.0	0.0
$CH_4^{\cdot +}$	C_{2v}[b]	C—H(α)	1.074	1.094	0.020
11	(55)	C—H(β)	1.169	1.204	0.035
		H(α)CH(α)	124.0	116.8	−7.2
		H(β)CH(β)	56.0	62.4	6.4
C_2H_3		C—H(α)	1.083	1.050	−0.033
12		C—H_{cis}	1.085	1.091	0.006
	C_S[b]	C—H_{trans}	1.083	1.092	0.009
	(52)	C—C	1.357	1.308	−0.049
		CCH(α)	130.8	171.7	40.9
		CCH_{cis}	122.3	123.3	1.0
		CCH_{trans}	121.4	122.4	1.0
C_2H_5		C—H(α)	1.093	1.083	−0.010
13		C—H(β)	1.104	1.111	0.007
	C_S[a]	C—H(β)*	1.113	1.112	−0.001
	(53)	C—C	1.512	1.475	−0.037
		CCH(α)	121.5	121.5	0.0
		CCH(β)	111.0	111.7	0.7
		CCH(β)*	113.0	110.9	−2.1
$C_2H_6^{\cdot +}$		C—H*	1.131	1.156	0.025
14		C—H	1.081	1.102	0.021
	C_{2h}, $^2A_1$[b]	C—C	1.579	1.591	0.012
	(54)	CCH*	82.6	86.5	3.9
		HCH	115.8	112.0	−3.8
		CCX	143.3	141.1	−2.2
cyclo-$C_3H_6^{\cdot +}$		C—H(α)	1.074	1.092	0.018
		C—H(β)	1.078	1.110	0.032
15	C_{2v}, $^2A_1$[a]	C(α)—C(β)	1.477	1.490	0.013
	(55)	HC(α)H	118.0	116.6	−1.4
		HC(β)H	115.4	108.8	−6.6
		CC(β)C	78.8	83.4	4.6
		C(β)C(α)X	178.9	175.0	−3.9
$C_3H_8^{\cdot +}$		C—H(t*)	1.121	1.133	0.012
16		C—H(t)	1.087	1.103	0.016
	C_{2v}, $^2B_2$[b]	C—H(c)	1.088	1.107	0.019
	(31)	C—C	1.576	1.592	0.016
		CCH(t*)	92.1	94.0	1.9
		CCH(t)	114.3	114.3	0.0
		H(t*)CH(t)	110.4	110.9	0.5
		H(c)CH(c)	112.3	109.7	−2.6
		C(t)C(c)C(t)	94.4	98.4	4.0

Note. I is the "certain" geometry for **9**, **11**—**16** determined by nonempirical calculations in type 6-31 G* basis sets (for **12**, in the STO-3G basis set) or from experiment (for **10**). II is the geometry optimized by MNDO-UHF, Δ are deviations of the geometric parameters of II from I.
[a] π-Radical **9**, **10**, **13**, and **15**. [b] σ-Radicals: **11**, **12**, **14**, and **16**.

In spite of fairly uncertain C—H distances (radical cations **11** and **14**—**16**), the bond angles (II) optimized by the MNDO-UHF method are rather close to the reliable values (I) (see Table 2). The unusually great deviation of the Δ(C—C—H(α)) bond angle for the $HC{=}CH_2$ σ-radical **12** is most likely due to its relatively low symmetry (C_S). The data of Table 2 indicate that the MNDO-UHF method makes it possible to calculate bond angles in free radicals more accurately than chemical bond lengths and that the reliability of the calculations of the structural parameters substantially increases as the symmetry of the radical increases.

Approbation of the AMNDO-UHF method

In the context of the AMNDO-UHF approach, the conversion of the spin populations ρ_s^H into the a^H_{iso} IHFC constants (Eq. (1*)) is carried out using two structurally and chemically determined proportionality coefficients, K(H(α)) and K(H(β)), rather than one averaged coefficient (for example, K(H) = 508 Oe[29]). The values of these coefficients are mostly stipulated by the type of free radical (π or σ, see Refs. 28, 29) and the nature of the "heavy" atom (C, N, O, *etc.*) bearing the proton. For hydrocarbon RC, K(H(α)) = 415 Oe, K(H(β)) = 850 Oe, and K(C)= 650 Oe proved to be optimal.

When the reliable geometry and the above-mentioned K(Z) values are used, the general agreement of the IHFC constants calculated in the AMNDO-UHF approximation (see Table 3) with experimental a^Z_{iso} is quite satisfactory (coefficients of correlation: r^H = 0.973 and r^C = 0.986). However, the IHFC constants with the H(α) and C(β) nuclei in the low-symmetry (C_s) C_2H_3 radical determined in the context of AMNDO-UHF are still substantially different from the experimental data. A similar deviation (Δa^H_{iso} = −16.3 Oe) from the experimental value was observed for the H* β-proton in the $C_2H_6^{\cdot +}$ radical cation. It is noteworthy that AMNDO-UHF calculations result in substantial errors in the IHFC constants with exactly those protons (H(β) in $CH_4^{\cdot +}$, H(α) in C_2H_3, and H* in $C_2H_6^{\cdot +}$) for which the energy optimization in the context of MNDO gave great deviations Δ (see Table 2) between the found and reliable values for C—H bond lengths (0.035, −0.033, and 0.025 Å, respectively).

The presence of two proportionality coefficients, K(H(α)) and K(H(β)), in the AMNDO-UHF scheme eliminated the apparent contradiction between previous recommendations,[50,61] according to which, in the framework of the MNDO-UHF calculations, one should decide between using K(H(α)) = 504.5 Oe[50] and K(H) = 850 to 900 Oe.[61] The majority of the previously considered[50] free radicals are of the π-type, and characterized above all by moderate (|20—30| Oe) negative a^H_{iso} values. On the other hand, Glidewell[61] discussed predominantly σ-type free-radical systems (radical cations

Table 3. The a^{Z}_{iso} IHFC constants (Oe) of neutral and charged hydrocarbon radicals

Radical	Reference	Nucleus Z_n	Experiment	*ab initio*	MNDO-UHF		AMNDO-UHF
$CH_2^{\cdot -}$		H	−16.0	−15.7	−19.3	−19.7	−16.1
9	53	C	21.1	14.3	45.9	44.0	25.3
CH_3		H	−23.0	−23.4	−27.7	−27.6	−22.6
10	52, 59	C	38.3	27.3	63.9	63.7	36.7
$CH_4^{\cdot +}$		H(α)	−14.6	−11.1	−14.8	−15.8	−12.9
11	55, 15, 60	H(β)	121.7	116.2	110.5	97.8	163.6
		H_{cp}	54.8	52.6	49.4	41.0	68.6
		C	—	8.9	23.3	29.1	16.7
C_2H_3		H(α)	13.4	−1.3	−31.8	−10.3	−8.4
12	59	H_{cis}	37.0	42.8	42.8	23.4	39.1
		H_{trans}	65.0	62.4	38.0	43.5	72.7
		C(α)	107.6	139.3	93.5	183.8	106.1
		C(β)	−8.6	−16.4	−40.3	−39.5	−23.2
C_2H_5		H(α)	−22.4	−25.4	−27.3	−27.6	−22.6
13		H(β)	26.9	20.8	19.3	11.4	19.0
	58*	C(α)	39.1	39.3	67.8	65.2	37.5
		C(β)	−13.6	−13.2	−10.4	−10.4	−6.0
$C_2H_6^{\cdot +}$		H*	152.5	131.3	85.3	81.4	136.2
14		H	−9.0	−8.8	−8.4	−8.4	−6.9
	57	C	—	—	12.5	15.1	8.7
cyclo-		H(α)	−12.5	−12.3	−13.7	−12.3	−10.0
$C_3H_6^{\cdot +}$		H(β)	21.0	16.5	10.5	9.1	15.3
15	61	C(α)	—	18.3	28.1	26.6	15.3
		C(β)	—	−13.2	−7.2	−20.4	−11.8
$C_3H_8^{\cdot +}$		H(t*)	98.0	90.0	54.0	55.5	92.9
16		H(t)	—	—	−6.5	−6.2	−5.1
	31	H(c)	—	—	−8.1	−8.1	−6.6
		C(t)	—	—	7.8	11.0	6.3
		C(c)	—	—	3.4	6.0	3.5

* Average values for the H(β) protons.

derived from ethers and acetals) with large (40—160 Oe) positive IHFC constants with the protons peculiar to such systems.

These characteristic features of π- and σ-electron radicals are known[29] to reflect the domination of the polarization (π) or delocalization (σ) mechanism of the appearance of the spin density on their protons, respectively. In this connection, the opinion has been stated[62] that in the context of semiempirical calculations like MNDO, it is correct to use two proportionality coefficients, $K(H(\alpha))$ and $K(H(\beta))$.

The introduction of the second coefficient is most likely required only to correct the spin densities, ρ_s^H, calculated in one or the other approximation (in the case of MNDO-UHF, probably only those with a positive sign), whereas, in fact, $K(H(\alpha)) = K(H(\beta))$.[62]

In order to increase the efficiency and correctness of the calculations of the a^{H}_{iso} IHFC constants by MINDO/3,[63] MNDO,[50] and AM1[62] methods, we used the previously[64] suggested scheme for annihilation of the extrinsic quartet component, which converted the ψ^{UHF} wave function into the ψ^{AUHF} function with a corrected doublet character.[29] As this was done, the coefficients of proportionality, $K(H(\alpha))$ and $K(H(\beta))$, in fact became equal to one another. The averaged $K(H(\alpha))/K(H(\beta))$ ratios for the MINDO/3-AUHF, MNDO-AUHF, and AM1-AUHF methods were 0.783, 1.293, and 1.013, respectively, and in the latter case an extremely high correlation coefficient, $r^H = 0.999$, was reached.[62]

Although AM1-AUHF[62] clearly stands out among the above-listed approximations by the unexpectedly good $K(H(\beta))/K(H(\alpha))$ and r^H values, this fact should be treated with particular caution for several reasons. First, it is unlikely that the experimental IHFC constants with nonhydrogen nuclei, Z = C, N, O, could be simulated with the same accuracy even for an appropriately selected series of similar radicals, for which $r^H = 0.999$. For example, it has been reported[50] that on going from MNDO-UHF to MNDO-AUHF, the r^C correlation coefficient decreases from 0.923 to 0.773, whereas r^H increases from 0.627 to 0.899, *i.e.*, one correlation (for ^{13}C) deteriorates as the other correlation (for ^{1}H) improves.

Second, the ability of the AM1 scheme to reliably determine the certain geometric parameters of free radicals also requires extensive verification. It should be noted that the angle of twist of the methylene groups in $C_2H_4^{\cdot+}$ optimized[37] in the context of AM1 (44.6°) was almost twice the experimental angle (25°). In addition, one may refer to the recent example of the $C_2H_6^{\cdot+}$[65] radical cation whose electron structure in the ground state was miscalculated in the AM1 approximation (unlike MNDO-UHF).

However, the main reason one should have a watchful attitude toward the AM1-AUHF method is associated with the recommendation[62] that $K(H(\alpha)) = K(H(\beta)) = 1177$ Oe be used to evaluate the IHFC constants with protons. In our opinion, it is unlikely that any noncontradictory argument could be found in favor of this great deviation of $K(H(\alpha))$ and $K(H(\beta))$ from the $K(H) = 508$ Oe value for a free atom.[29] The same relates to the MNDO-AUHF method where $K(H) = 1206$ Oe[50] is used. On the other hand, the clear-cut orientation of the AMNDO-UHF scheme to the use of two proportionality coefficients ($K(H(\alpha)) = 415$ Oe, $K(H(\beta)) = 850$ Oe) and the common practice of using only one value ($K(H) = 539.86$ Oe)[29] in the framework of INDO-UHF force one to turn to the problem of determining the spin density, ρ_s^H, using NDO-UHF methods.

The ρ_s^H spin densities. The relationships and properties of the ρ_s^H spin densities that directly relate to the ψ^{UHF} one-determinant wave function and to the completely projected wave function (ψ^{PUHF}) or to the wave function that has undergone annihilation of only the extrinsic quartet component (ψ^{AUHF}) have been discussed in detail previously.[29] It is known that ψ^{UHF} is not an eigenfunction of the operator of the total spin $\hat{S}^2$, *i.e.*, it contains extrinsic components with higher multiplicities, whose contributions to ρ_s^Z vary disproportionately in the transition from the ground state to vibration excited states. For example, ψ^{UHF} for the NH_2 radical in which the chemical bonds are 60 % longer (than the equilibrium bonds), contains the doublet and quartet components in equal parts, though in the original ground state, the former predominates.[29]

Taking this into account, the drive to find guaranteed improvements of the spin properties of ψ^{UHF} by any simple method is quite natural. However, systematic monitoring using the extended Hartree—Fock method (EHF), where the variation principle is applied directly to the multi-determinant wave function ψ^{PUHF}, showed a number of theoretical and practical drawbacks inherent in the procedures of the ψ^{UHF} projected or removal of the quartet component from it, which are usually carried out after minimization of energy. In particular,[29] it has been noted that, due to the tendency of the UHF approach to overestimate the spin polarization effects caused by the electron correlation, they really need to be decreased somehow, in order to correctly calculate the IHFC constants. However, in the schemes that involve removal of the extrinsic components, the role of spin polarization is usually understated, and sometimes to too great an extent. Therefore, it is difficult to predict which of the approximate spin densities ($^{UHF}\rho_s^H$, $^{PUHF}\rho_s^H$, or $^{AUHF}\rho_s^H$) will be closer to the more precise value ($^{EHF}\rho_s^H$).

The fact[50,62] that the optimal proportionality coefficients $K(H)$ that correspond to the MINDO/3, MNDO, and AM1 versions are approximately doubled after annihilation of the extrinsic quartet component in ψ^{UHF}, indicates unambiguously that the contribution of the spin-polarization effects decreases inordinately. From this it follows that for the quantum-chemical analysis of the constants of IHFC with protons it is more expedient to use the above-mentioned semiempirical approximations combined with the UHF approach. The same is indicated by the experience accumulated on the use of the INDO method for evaluation of the ESR parameters of free radicals,[29] which implies that, in conformity with the theoretical views, $^{UHF}\rho_s^H$ is only slightly greater than $^{EHF}\rho_s^H$, while $^{AUHF}\rho_s^H$ is substantially smaller than $^{EHF}\rho_s^H$.

The assumption that $K(H)$ depends on the mechanism of the distribution apparently reflects a feasible division[29] of the majority of free radicals detected into two symmetry classes, π and σ. Actually, Nelsen[62] reported the easiest method, which makes it possible to depict indirectly the specific character of the two above-mentioned mechanisms using the set of $K(H(\alpha)) = 387.9$ Oe and $K(H(\beta)) = 784.3$ Oe formally introduced for AM1-UHF.

In fact, according to the method of hybridization of the basis (MHB), the one-electron contributions to the IHFC constants with protons in organic radicals are approximately determined from relationships (2*)—(4*):[29]

$$a_0^H = 508 \cdot \rho_0^H, \text{ (Oe)}, \qquad (2^*)$$

$$\rho^H{}_0 = C_{2h} \cdot \xi^3(H), \qquad (3^*)$$

$$\xi(H) = \left(1 + \frac{3}{8} \cdot S^2 + \frac{35}{128} \cdot S^4\right)^{2/3}, \qquad (4^*)$$

$$a_{iso}^{H(\alpha)} = K(H(\alpha)) \cdot \rho_s^{H(\alpha)}, \ (\rho^{H(\alpha)} < 0), \qquad (5^*)$$

$$a_{iso}^{H(\beta)} = K(H(\beta)) \cdot \rho_s^{H(\beta)} = [K(H(\alpha))] \cdot (\xi^3(H) \cdot \rho_s^{H(\beta)}), \qquad (6^*)$$

$$(\rho^{H(\alpha)} < 0),$$

where C_h is the coefficient at the hydrogen AO symmetrically orthogonalized according to Löwdin in the expression for the unpaired electron MO, and $S = \langle \sigma_C | S_H \rangle$ is the overlap integral relating to the C—H chemical σ-bond. As a rule, for typical cases, the deviations from $S = 0.75$ are small, which correlates, according to (1*)—(4*), with $\xi(H) \approx 1.2$ and $K_0(H(\beta)) = 508\xi^3(H) \approx 860$ Oe. Relationships (2*)—(4*) are inapplicable to

purely π-electron radicals, since C_h is always 0, and, therefore, the contribution of the exchange polarization mechanism (a_{ep}^H) to the a^H_{iso} constant becomes the only one.[29] Taking the foregoing into account, it is quite possible that with $K(H(\alpha))$ = 415 Oe, the widely used versions of NDO-UHF can provide satisfactory accuracy in the evaluations of the constants of IHFC with protons in π-electron hydrocarbon radicals.

On the other hand, the above-determined $K(H(\beta))/K(H(\alpha))$ = 850/415 = 2.1 ratio for hydrocarbon radicals in the AMNDO-UHF scheme can be interpreted in a theoretically acceptable way by taking into account the fact that the MNDO approximation as a modification of NDDO appears to be mathematically and physically justified[29] in the Löwdin symmetrically orthogonalized basis, which is, in the authors' opinion, represented by Eqs. (2*)—(6*). Then for $K(H(\alpha))$ in (5*) and $K(H(\beta)) = K(H(\alpha))\xi^3(H)$ in (6*), at $\xi \simeq 1.28$, the $K(H(\beta))/K(H(\alpha))$ ratio is automatically 2.1. By interpreting ξ^3 as a scale factor, which modifies the spin population, ρ_s^H, we obtain the single coefficient of proportionality, $K(H)$, in relationships (5*)—(6*).

The contribution of delocalization to the spin densities at the protons in the σ-electron radicals predominates,[29] and its evaluation by standard NDO versions requires the introduction of the $\xi^3(H)$ scale factor (ξ = 1.2 to 1.3; see Ref. 51, 58), which means returning from the symmetrically orthogonalized basis to the usual atomic basis (see Eqs. (2*)—(4*)). This is actually reflected by the form of the right-hand side of Eq. (6*). Unfortunately, this intrinsically noncontradictory approach to the determination of the HFC constants of free radicals has not yet been widely approved.

Thus, there are good theoretical reasons for using two proportionality coefficients, $K(H(\alpha))$ and $K(H(\beta))$, in the quantum-chemical analysis of IHFC with protons in π- and σ-electron radicals in the context of AMNDO-UHF. Actually, the semiempirical evaluation of the a^H_{iso} constants is carried out with one $K(H)$ value equal to 415 Oe (see Eqs. (5*)—(6*)), and the scale factor, ξ = 1.28, is only used for the conversion of the ρ_s^H spin populations calculated from the Löwdin symmetrically orthogonalized basis into the standard atomic basis.

Eqs. (3*) and (4*), in spite of their simplified form, reflect the fact that in the MO LCAO approximation, the spin densities on the atomic nuclei in free radicals are determined *via* the overlap integrals of the AO. For protons, those $S_{\sigma h}$ overlap integrals that relate to the C—H, N—H, O—H, *etc.* chemical bonds are normally the most significant. Since the $S_{\sigma h}$ values sometimes differ rather considerably from one another, it is not surprising that good agreement between the calculated and experimental a^H_{iso} values is not always achieved using a single conversion coefficient (for example, $K(H(\alpha))$ = 508 Oe[29]).

In fact, when the reliable geometry and $K(H(\alpha))$ = 508 Oe are used in the context of MNDO-UHF, the constants of IHFC with the protons in the CH_3 radical are overestimated (−27.6 Oe instead of −23.0 Oe), while those in the $NH_3^{\cdot+}$ and $H_2O^{\cdot+}$ radical cations are underestimated (−22.9 Oe and −15.9 Oe instead of −25.9 and −26.1 Oe, respectively).[28] This is also an argument in favor of the individual determination of $K(H(\alpha))$ for chemical bonds of different types, C—H, N—H, O—H, *etc.* It should be noted that Glidewell,[67] who analyzed the constants of IHFC with protons attached to C or S atoms by the MNDO-UHF method, arrived at the same conclusion.

The geometry of hydrocarbon RC. For the reliable AMNDO-UHF calculation of the constants of IHFC with protons in hydrocarbon free radicals, the structural parameters corresponding to the reliable geometry should be used, along with the two proportionality coefficients ($K(H(\alpha))$ = 415 Oe and $K(H(\beta))$ = 850 Oe). This relates most of all to C—H bond lengths. However, the geometries of complex free radicals are, as a rule, unknown, and the present-day semiempirical methods like MNDO determine these geometries with unacceptably great errors, especially for low-symmetry radical systems. Therefore, while determining the constants of IHFC with protons in primary and distonic $VCP^{\cdot+}$ ($C_5H_8^{\cdot+}$) with C_1 or C_S, symmetry in the context of AMNDO-UHF, one cannot rely on structural parameters preliminarily optimized by MNDO.

Simple methods for the selection of an adequate geometry of hydrocarbon RC based on easily accessible structural data on related molecules and on ESR data on the magnetic-resonance interactions in structurally similar RC may be suggested as an alternative. It should be taken into account that typical σ-electron radicals normally have positive spin densities ($\rho^{H(\beta)}>0$) at protons, which is reflected in the $\rho^{H(\beta)}$. On the other hand, the α-protons in the standard π-electron radicals possess negative spin densities ($\rho^{H(\alpha)}$).

Simultaneous analysis of available radiospectroscopic and structural data indicates that the C—H(β) and C—H(α) chemical bonds in hydrocarbon RC are usually longer and shorter, respectively, than their analogs in related nonionized hydrocarbons. For example, according to *ab initio* calculations in an extended basis of the type 6-31 G** with consideration for the electron correlation,[30,68] all of the C—H bonds in nonbranched and branched alkanes are characterized by tetrahedral hybridization of the carbon atom ($C(sp)^3$—H) and nearly identical lengths (1.086 Å). After ionization of alkanes, those C—H(β) bonds whose protons acquire high positive spin densities become much longer (specifically, by 0.045 Å with $a^{H(\beta)}_{iso}$ = 152.5 Oe for $C_2H_6^{\cdot+}$ (C_{2h})[30]). In the case of especially large (50—250 Oe) a^H_{iso} constants, the C—H(β) bond lengths in hydrocarbon RC can be adequately evaluated by methods that we will not consider here,* since they have not been extended to $VCP^{\cdot+}$.

* A separate communication will be devoted to this problem.

The C—H bonds in cyclopropane, ethylene, and VCP, which has a similar structure, are 0.01 Å shorter than those in nonbranched and branched alkanes, and the (H—C—H) bond angles between them are 115—117° (see Refs. 69, 70). Therefore, these may be assigned to C(sp)^2—H type bonds. The α-protons in this type of bond in RC (including those in *anti*-VCP$^{\cdot+}$) are located in the nodal planes of the unpaired electron MO and are generally characterized by negative IHFC constants moderate in magnitude: $|a^{H}_{iso}| \leq 23$. On the other hand, reliable *ab initio* calculations[10,30] for a number of hydrocarbon RC including $C_3H_6^{\cdot+}$ (C_{2v}) have shown that the C(sp)^2—H(α) bonds in these RC are practically identical to those in the original molecules and, in some cases, they are even shorter (by 0.005 Å).

Taking the foregoing into account, one may assume that the lengths of those C—H chemical bonds whose α- and β-protons have weak or even moderate IHFC (0—30 Oe) with the unpaired electron in the resulting RC, do not increase noticeably upon ionization of the hydrocarbons. In these cases, it is expedient to use certain experimental and theoretical data on the interatomic distances in related molecular systems for the AMNDO-UHF quantum-chemical analysis of the magnetic-resonance parameters of hydrocarbon RC. The efficiency of these methods for selecting the geometry of free radicals in the cases of INDO and CNDO methods has been clearly demonstrated in many works.[29]

The analysis of IHFC in primary and distonic VCP$^{\cdot+}$ by the AMNDO-UHF method

According to the ESR data, the vinyl groups in *anti*- and *gauche*-VCP$^{\cdot+}$, unlike the cyclopropane rings, are characterized by similar a^{H}_{iso} constants (see Table 1). Therefore, it is reasonable to assume that the geometries of the vinyl fragments in *anti*- and *gauche*-VCP$^{\cdot+}$ are nearly identical. At the same time, the conformational angles τ between the axis of the C=C bond of the vinyl group and the bisectrix of the adjacent C—C—C angle of the cyclopropane ring in these RC and also in their molecular precursors are apparently substantially different (Scheme 7).

Scheme 7

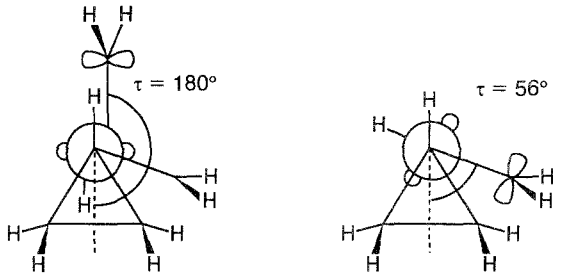

anti-VCP *gauche*-VCP

In the case of the *anti*-conformation of the VCP or the corresponding RC, the τ angle is precisely 180°, whereas in the similar *gauche*-conformers it is not defined so stringently. It is not inconceivable that the adiabatic ionization of the *gauche*-VCP molecule is accompanied by some deviation from the typical τ = 56°. Therefore, the conformational angle τ in *gauche*-VCP$^{+\cdot}$, unlike other structural parameters, was additionally varied over the 60—90° interval (Table 4).

As was stressed above, in the case of low-symmetry hydrocarbon radicals, the preliminary MNDO-UHF procedure of the energetic optimization of their geometry often proves to be unsatisfactory, since the structural parameters are unsuitable for the subsequent correct AMNDO-UHF evaluation of the a^{Z}_{iso} IHFC constants (Z = ^{1}H, ^{13}C) with satisfactory accuracy. *Anti*- and *gauche*-VCP$^{\cdot+}$ have low symmetries (C_S and C_1, respectively), but are, however, characterized by rather small $|a^{H}_{iso}|$ values of ≤ 30 Oe. Therefore, in conformity with the foregoing, for the AMNDO-UHF calculation of the a^{H}_{iso} constants of both RC, the same geometry of the *anti*-VCP molecule (except for τ) preliminarily optimized in the MNDO-UHF approximation was used.

Table 4. The a^{Z}_{iso} constants of IHFC (Oe)[a] with protons for primary radical-cations VCP$^{+\cdot}$ depending on the conformational angle τ calculated by the AMNDO-UHF method[b]

Proton[c]	*gauche*-VCP$^{\cdot+}$							*anti*-VCP$^{\cdot+}$
	60°	65°	70°	75°	80°	85°	90°	180°
2H(5)	−12.2	−12.2	−12.2	−12.2	−12.1	−12.1	−12.1	−12.4
H(4)	−7.0	−7.2	−7.6	−7.9	−8.2	−8.4	−8.5	−5.2
H(1)	20.2	23.1	26.0	28.4	30.4	31.7	32.1	−1.1
H(2*)	1.5	1.3	0.8	0.3	−0.1	−0.4	−0.7	−0.1
H(2)	1.5	1.3	0.8	0.3	−0.1	−0.4	−0.7	1.9
H(3*)	−1.4	−1.4	−1.4	−1.3	−1.1	−0.9	−0.7	−0.1
H(3)	−1.4	−1.4	−1.4	−1.3	−1.1	−0.9	−0.7	1.9

[a] See Scheme 7. [b] The scheme of the calculation is given in the text. [c] See Scheme 5.

When the conformational angle τ in *gauche*-$VCP^{\cdot+}$ was varied, the best agreement between the AMNDO-UHF-calculated and experimental a^{H}_{iso} constants (see Table 4) ($|a(2\ H(5))| = 13.0$ Oe, $|a(1\ H(4))| = 7.3$ Oe, $|a(1\ H(1))| = 26.0$ Oe, see Table 1) was achieved at $\tau = 70°$ (recall that $\tau = 56°$ for *gauche*-$VCP^{\cdot+}$). The a^{H}_{iso} values for *anti*-$VCP^{\cdot+}$ calculated by AMNDO-UHF (see Table 4) are also close to the experimental data: $|a(2\ H(5))| = 13.0$ Oe, $|a(1\ H(4))| = 7.3$ Oe, and $|a(1\ H(1))| = 2.7$ Oe (see Table 1). Thus, the AMNDO-UHF calculations of the a^{H}_{iso} IHFC constants carried out by us confirm the previous[4] assignment of the ESR spectra of *anti*- and *gauche*-$VCP^{\cdot+}$ and are a testimony to the above-stated views of the structural features of the two isomeric forms of $VCP^{\cdot+}$.

It follows from the analysis of the ESR spectra that the distributions of the unpaired electron and the positive charge in the distonic RC, *dist*(90.0)- and *dist*(0.90)-$C_5H_8^{\cdot+}$ (**4** and **3**, respectively), are nearly identical. In both RC, the locations of the spin density and the positive charge are almost entirely separated; the unpaired electron and the positive charge are predominantly located at the terminal groups, $^{\cdot}C(\alpha)H_2$ and $^{+}C(\gamma)HR$, respectively (Scheme 8). The single-occupied molecular orbital (SOMO) in RC **4** or **3** belongs almost completely to the $C(\alpha)H_2$ and $C(\beta)H_2$ methylene fragments, while the lowest unoccupied molecular orbital (LUMO) belongs to the conjugated neighbors, $^{\cdot}C(\beta)H_2$ and $^{+}C(\gamma)HR$.

Scheme 8

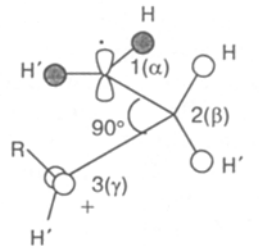

17: R=H, *dist*(90,0)-$C_3H_6^{\cdot+}$ (C_s)
4: R=$CHCH_2$, *dist*(90,0)-$C_5H_8^{\cdot+}$ (C_1)

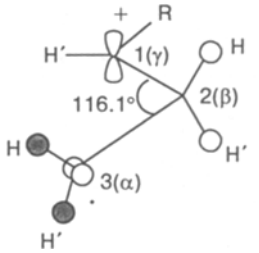

18: R=H, *dist*(0,90)-$C_3H_6^{\cdot+}$ (C_s)
3: R=$CHCH_2$, *dist*(0,90)-$C_5H_8^{\cdot+}$ (C_s)

Although the compositions of the SOMO and LUMO in RC **4** and **3** are nearly identical, the $^{\cdot}C(\alpha)H_2$ and $^{+}C(\gamma)HR$ terminal methylene groups have different orientations with respect to the central fragment $C(\beta)H_2$. In fact, in RC **4**, the p-AO of the $^{\cdot}C(\alpha)H_2$ group occupied by the unpaired electron is arranged across (at a right angle to) the C(α)—C(β)—C(γ) plane, and in RC **3**, it is arranged along this plane (see Scheme 8). Unlike this AO, the electron-deficient p-AO of the positively charged $^{+}C(\gamma)HR$ group in RC **4** is directed along the above-mentioned plane, and in RC **3** it lies across this plane.

The distinctions in the conformations of RC **4** and **3** are manifested in the spectra as different splittings on the β-protons: 30.4 and 14.7 Oe, respectively (see Table 1). For the distonic RC derived from the unsubstituted cyclopropane detected in Freon-113 at 108 K by ESR, the splittings on the β-protons are known[6] to be 30.2 Oe. Thus, in this case, the *dist*(90.0)-$C_3H_6^{\cdot+}$ conformer (**17**) is realized (see Scheme 8).

It should be stressed that the magnetic-resonance parameters for RC **17** and **4** virtually coincide, despite the fact that the positively charged center in RC **4** is additionally stabilized by the substituent R = $CHCH_2$. This means that the distribution of the spin populations in RC **17** and **4** and also the structural features of their trimethylene systems are similar. Therefore, for the sake of simplicity we shall restrict our further consideration to the distonic RC **17**, since its trimethylene fragment should possess the same geometric and electronic structure as that in RC **4**.

No distonic RC of unsubstituted cyclopropane with a different configuration of the atoms that is peculiar to the *dist*(90.0)-$C_3H_6^{\cdot+}$ (**18**) conformer (see Scheme 8) has been so far detected by ESR. However, there are arguments that indicate that the trimethylene systems in RC **18** and **3** as well as those in RC **17** and **4** are isostructural and isoelectronic. Because of this, the corresponding splittings on the β-protons in the ESR spectra are practically identical. Thus, it is quite reasonable that the β-protons in RC **18** be characterized by the splitting of 14.7 Oe observed in the case of RC **3**, since for a similar pair of RC, **17** and **4**, no redistribution of the spin densities was detected by ESR as H in the positively charged $^{+}C(\gamma)H_2$ group was replaced by $CHCH_2$. Moreover, the distonic RC **7** and **8** (derived from tri- and tetramethyl substituted cyclopropane, respectively) with the *dist*(0.90)-conformation of the trimethylene fragment exhibit only slightly smaller splitting on the β-protons (11.7 Oe, see Table 1), which is accounted for by partial electron transfer to the methyl substituents at the radical center.

One should also bear in mind the conformational similarity between the distonic **3**, **4**, **17**, and **18** and β-substituted derivatives of the ethyl radical, $^{\cdot}C(\alpha)H_2C(\beta)H_2Z$ (Z is Me, NH_2, OH, F, SiH_3, PH_2, SH, or Cl), with rather rigidly fixed configurations of the atoms.[71] In particular, when Z is Me, NH_2, OH, or

F structural similarity with the *dist*(90.0)-$C_3H_6^{\cdot+}$ **17** and *dist*(90.0)-$C_5H_8^{\cdot+}$ **4** RC is observed, and when Z is SiH_3, PH_2, SH, or Cl, there is similarity with *dist*(0.90)-$C_3H_6^{\cdot+}$ **18** and *dist*(0.90)-$C_5H_8^{\cdot+}$ **3** RC. It is noteworthy that for a number of substituents Z containing "heavy" atoms only from Period II or only from Period III of the periodic table, the splittings on the β-protons in $^{\cdot}C(\alpha)H_2C(\beta)H_2Z$ are rather close to each other and lie in the 25.6—30.3 Oe or 13.5—17.1 Oe interval, respectively, (except for Z = Cl when $a^{H(\beta)}_{iso}$= 10.2 Oe).[71]

In view of the low sensitivity of the spin distribution to the nature of the β-substituent Z in the above-mentioned series of isoelectronic derivatives $^{\cdot}C(\alpha)H_2C(\beta)H_2Z$, it is unlikely that γ-substitution, which transforms RC **17** and **18** into RC **3** and **4**, respectively, by replacement of the H atom by the $CH{=}CH_2$ group, would substantially affect the structural and radiospectroscopic parameters of the trimethylene fragment in the $^{\cdot}C(\alpha)H_2C(\beta)H_2{}^{+}C(\gamma)HR$ distonic RC (see Scheme 8). In this case, quantum-chemical analysis of the ESR spectra of distonic RC **3** and **4** is considerably simplified, since one may use only information on the geometric and electronic structures of conformers **17** and **18**.

While comparing the *dist*(90.0) and *dist*(0.90) conformers, one can easily see (see Scheme 8) that RC **17** and **18** possess identical symmetry, C_S, while RC **4** and **3** have distinct symmetries, C_1 and C_S, respectively. At the same time, all of these distonic structures, like the preceding cyclic radical forms **1**, **2** ($C_5H_8^{\cdot+}$), and **15** ($C_3H_8^{\cdot+}$), are characterized by uniformly moderate IHFC constants, $|a^H_{iso}| \leq 30$ Oe (see Tables 1, 3). Therefore, for the predetermination of the structural parameters for all seven of the RC listed in the context of AMNDO, one should seemingly be guided by the same rules (see above).

However, the uniform approach to the preliminary selection of the geometry of the above-mentioned paramagnetic particles is impossible, because of the fundamental distinction between the secondary RC, **3, 4, 17, 18**, and the primary RC, **1, 2, 15**. In fact, while each of the primary cyclic RC correlates with the particular molecule from which it has been directly formed by ionization, for any of the secondary distonic RC this direct correlation is excluded, and, therefore, the structural data necessary for reliable AMNDO-UHF evaluations of the magnetic-resonance parameters are almost always missing. Therefore, the known geometry of the starting C_5H_8 molecule is quite plausible as the reliable geometry of *gauche*- and *anti*-$VCP^{\cdot+}$ (**1** and **2**), whereas for distonic RC **17** and **18**, an equivalent alternative should be chosen by examining structurally similar fragments in well-studied related systems.

The formation of distonic RC **17** and **18** may be described rather conditionally but clearly by Scheme 9: the cyclopropane ring of the C_3H_6 molecule is cleaved initially to give a diradical, and then an electron is removed from one of its terminal atoms (C(1) or C(3)). The methylene groups in the diradical are oriented in the same manner as those in RC **17** and **18**. The mutually orthogonal arrangement of the planes of the C(1)—H_2 and C(3)—H_2 terminal fragments ensures the practically complete spatial separation of the two SOMO. During the one-shot ionization of the diradical, one of the SOMO loses the unpaired electron and becomes the lowest unoccupied molecular orbital (LUMO), while the other orbital remains singly occupied.

Taking Scheme 9 into consideration, it is easy to understand that the SOMO and LUMO in the distonic RC **17** and **18** (like those in the propyl radical, $^{\cdot}CH_2CH_2Me$, and its cation, $^{+}CH_2CH_2Me$[72]) are almost entirely built of the corresponding $2p_C$-AO of the terminal methylene groups. On the other hand, Scheme 9 reflects the structural similarity of these RC not to the original C_3H_6 molecule, but to its diradical form, the geometry for which is by no means more easily determined than that for the starting RC. Furthermore, the

Scheme 9

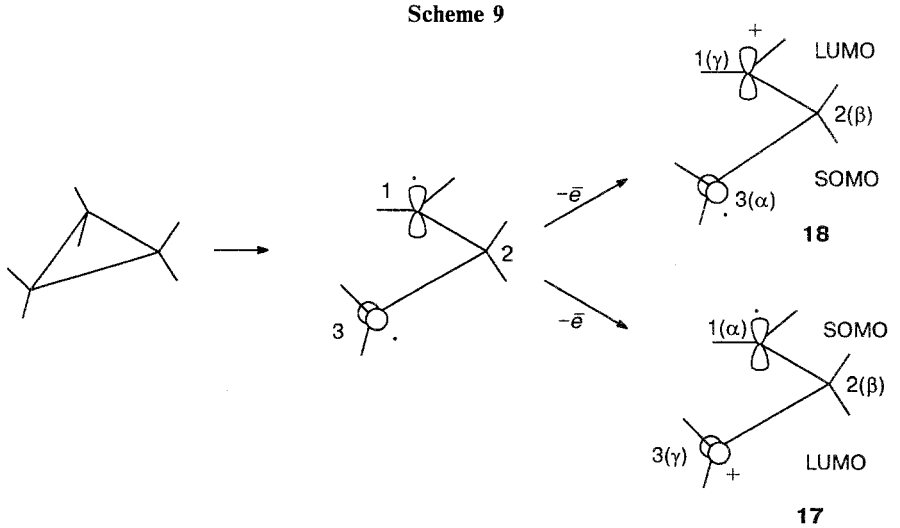

Table 5. The structural parameters of hydrocarbon molecules

Molecule	C—C—C/deg	C—C(C=C)*/Å	H—C—H′/deg	C—H(H′)/Å	Reference
C_2H_4	—	1.337(2)	117.2(1,2)	1.103(2)	74, 84
cyclo-C_3H_6	60.6	1.5139(12)	114.5(9)	1.0991(20)	85
cyclo-C_4H_8	87.6	1.554(1)	106.4(13)	1.109(3)	81
cyclo-$C_{10}H_{20}$	116.1(11)	1.545(3)	105.4	1.115(3)	83

* For C_2H_4.

same diradical precedes two dissimilar distonic RC (**17** and **18**), which indicates that the ionization of C_3H_6 involves an essential structural transformation.

Analogous changes in the geometric and electronic structures are also peculiar to other hydrocarbon systems with degenerate or nearly degenerate HOMO. In these cases ionization is accompanied by the removal of degeneracy, owing to the Jahn—Teller effect. The structural parameters of the resulting RC often deviate substantially from those existing in the original molecules (see **10**, **14—16** in Table 2). In order to take these deviations into account, it is most natural to turn to the generalized recommendation that involves fragment-for-fragment construction of hydrocarbon RC based on a set of "standard" structural components and known dependences between their geometric and electronic structures in well-studied molecules and free radicals.

As was noted above, distonic RC **17** and **18** possess formally dissimilar electronic configurations. This is manifested in the fact that the SOMO in RC **17** and **18** are built entirely of the AO of one terminal methylene group and the central methylene group, which are traditionally designated for the sake of convenience as $^{\cdot}C(\alpha)H_2$ and $C(\beta)(2)H_2$ (see Schemes 8 and 9). Only the AO of the $^{+}C(\gamma)H_2$ and $C(\beta)(2)H_2$ fragments contribute to the LUMO.

The fact that the electronic structures of the *dist*(90.0)- and *dist*(0.90)-$C_3H_6^{\cdot+}$ RC are different, while their topology is identical undoubtedly results from the noncoincidence of their geometric parameters. This applies most of all to the C(1)—C(2)—C(3) angle and the lengths of the C(1)—C(2) and C(2)—C(3) bonds (see Schemes 8 and 9). In fact, each of the terminal methylene groups ($C(1)H_2$ and $C(3)H_2$) contains an approximately $(sp)^2$-hybridized atom with such specific $C(sp)^2$—H bond lengths (~1.1 Å) and bond angles (115—117°) inherent in it, that their magnitudes are practically identical even in compounds that seemingly have little in common, such as ethylene and cyclopropane (Table 5). It is quite reasonable that the structural parameters of the $C(1)H_2$ and $C(3)H_2$ terminal fragments in distonic RC **17** and **18** (see Scheme 8) are also rather similar to those presented in Table 5 for C_2H_4 and *cyclo*-C_3H_6.

However, the central methylene group in $C(1)—C(2)H_2—C(3)$ needs special consideration. It must be taken into account that its local symmetry (C_{2v}) is much higher than the C_S-symmetry typical of RC **17** and **18**. This fact allows one to use the systematized[73—77] experimental data on the C—C—C and H—C—H bond angles and the C—C and C—H bond lengths that relate to $C—CH_2—C$ fragments having C_{2v} local symmetry in structurally similar neutral compounds. Although the geometric parameters of this fragment vary over wide limits (for example, 60—125° for C—C—C and 105—115° for H—C—H[73,74]), the variations observed are self-consistent: each of the C—C—C bond angles is matched by one set of the other three values (H—C—H, C—C, C—H).[73—77]

It is of interest that for cyclic hydrocarbons, all of the experimental values for the C—C—C angles in the $C—CH_2—C$ fragment (C_{2v}) are clustered around 60°, or 90°, or 113°.[73,74] On the other hand, the bond angles in the primary RC of cyclopropane ($^2A_1$) and two electronic states, $^2B_2$ and $^2B_1$, of propane with the same C_{2v}-symmetry are close to 80°, 92°, and 124°, respectively, as shown by reliable nonempirical calculations.[31,57] With this in mind and taking into account similar correlations of other geometric parameters, it is reasonable to assume that the structural regularities describing the $C—CH_2—C$ fragment of the C_{2v} symmetry experimentally determined[73—77] for molecules, are also valid for similar hydrocarbon RC. Therefore, all of the geometric parameters of the central methylene group, $C(2)H_2$, in distonic RC **17** and **18** can be readily evaluated from the values for the C(1)—C(2)—C(3) angles in structurally related neutral compounds.

In the series of cycloalkanes C_nH_{2n}, n = 3 to 10, built of $C—CH_2—C$ fragments with C_{2v} symmetry, the C—C—C angle increases from 60 to 116.1° as n increases from 3 to 10.[73—75] According to the data of photoelectron spectroscopy,[78—80] on going from n = 4 (C(1)—C(2)—C(3) = 87.6)[81] to n = 5 (C(1)—C(2)—C(3) = 104.4),[82] the arrangement of the two pairs of (quasi) degenerate HOMO changes. Therein lies the relationship between the character of the HOMO and the type of the above-discussed angle.

A similar angular dependence should be expected in the case of the SOMO of primary hydrocarbon RC containing the $C(1)—C(2)H_2—C(3)$ structural fragment with C_{2v} symmetry. In fact, *ab initio* calculations[31] showed that the SOMO in the propane RC (C_{2v}) in the $^2B_1$ electronic state is localized (like the HOMO in cyclobutane, where C(1)—C(2)—C(3) = 87.6°)[78—81] at the C—C chemical bonds, which correlates with a C—C—C angle of 92.1°. However, after transition of

this RC to the electronic state $^2B_1$, its HOMO is formed (like that in cyclopentane, C—C—C = 104.4°)[78,80–82] by C—H chemical bonds, and, consequently, the C—C—C bond angle increases from 92.1° to 124°.[31]

As was stressed above, it is useful to conditionally consider the diradical form (Scheme 9) where the 2p-AO of the C(3) and C(1) atoms, bearing the unpaired electrons, are conjugated with the C(1)—C(2) and C(2)—H chemical bonds, respectively, to be the structural precursor of the distonic hydrocarbon RC **17** and **18**. Considering this and also the above-noted similarity between the electronic structures of cyclobutane and the propane RC in the $^2B_2$ state, one should expect that the distonic RC **17** resulting from the removal of an electron from the orbital that is entirely localized at the C—C bonds will have a C—C—C bond angle close to 90°. Then all of the other geometric parameters of the $C(2)H_2$ central group in RC **17** can be evaluated by using the electron-diffraction data on gaseous cyclobutane (see Table 5).

For distonic RC **18**, in turn, the correlation with cyclodecane (n = 10), in which the C—C—C bond angle is 116.1° (see Table 5), is plausible.[83] This is due to the fact that for the last three representatives of the series of cycloalkanes C_nH_{2n}, n = 3 to 10, this angle is practically invariable and is equal to 116.1°,[73–75] *i.e.*, this magnitude is typical of an unstrained C—CH_2—C fragment with C_{2v} symmetry. In conformity with the foregoing, the electronic structure of this fragment may be considered to be virtually identical for cycloalkanes with $n \geq 5$ and for RC **18** resulting from the removal of an electron from the orbital conjugated with the C—H(β) bonds.

Table 5 summarizes the structural data obtained by gas electron diffraction[74,81,83–85] for the four molecules chosen by us to evaluate the geometry of the low-symmetry (C_S) distonic RC **17** and **18** (Table 6). The lengths of the C(1)—H, C(1)—H′, C(3)—H, and C(3)—H′ bonds and bond angles between them evaluated for RC **17** and **18** (see Table 6) are the averaged corresponding characteristics of ethylene and cyclopropane (see Table 5). Assuming the C—H and C—H′ bond lengths to be exactly identical, it is easy to determine that H—C(1)—C(2) = H′—C(1)—C(2) = 122° (see Table 6).

In conformity with the foregoing, the C(1)—C(2)—C(3) bond angle in RC **17** was taken to be 90°, and all of the geometric parameters of the $C(2)H_2$ central group were taken to be identical to those in cyclobutane (see Tables 5 and 6). The interatomic distances characterizing C(1)—C(2) and C(2)—C(3) in RC **17** were obtained as the average between the C=C bond length in ethylene and the C—C bond length in cyclobutane. The geometric parameters of distonic RC **18** (see Table 6) were evaluated in a similar way; however, structural data for cyclodecane, rather than for cyclobutane, were used (see Table 5).

Table 6. The geometry[a] of low-symmetry (C_s) and distonic $C_3H_6^{\cdot+}$ RC

Geometric parameter[b]	*dist*(90.0)-$C_3H_6^{\cdot+}$ (**17**)		*dist*(0.90)-$C_3H_6^{\cdot+}$ (**18**)	
	ab initio[c]	evaluation[d]	*ab initio*[c]	evaluation[d]
C(1)—C(2)—C(3)	92.7	90.0	118.0	116.1
C(1)—C(2)	1.571	1.446	1.445	1.440
C(2)—C(3)	1.423	1.446	1.496	1.440
H—C(1)—H′	120.0	116.0	120.0	116.0
H—C(1)—C(2)	113.5	122.0	120.0	122.0
C(1)—H(H′)	1.075	1.101	1.079	1.101
H—C(2)—H′	109.4	106.4	103.0	105.4
C(2)—H(H′)	1.081	1.109	1.102	1.115
H—C(3)—H′	120.0	116.0	120.0	116.0
C(3)—H(H′)	1.078	1.101	1.072	1.101

[a] Specification of the atoms is given in Scheme 8. [b] Bond angles are given in degrees, the lengths of chemical bonds are in Å. [c] UHF/6-31 G*.[10] [d] See the text.

In addition to the estimated values, Table 6 presents the values obtained by *ab initio* calculations in the 6-31 G* extended basis in the context of the UHF approximation.[10] As can be seen from Table 6 and Scheme 8, the greatest disagreement is observed for the C(α)—C(β) distance, which is equal to 0.125 Å for RC **17** and 0.056 Å for RC **18**. Non-coincidences of C—H bond lengths (0.02—0.03 Å) can also be noted. However, all of the bond angles evaluated by us and calculated *ab initio*,[10] except for H—C(1)—C(2) in RC **17**, are in a good agreement with each other.

The experimental and AMNDO-UHF-calculated constants of IHFC with the ^1H and ^{13}C nuclei in RC **17** and **18** are given in Table 7. The quantum-chemical calculations for these two distonic forms of $C_3H_6^{\cdot+}$ were carried out using the RC geometry either predicted *ab initio*[10] or evaluated by us (see Table 6). Along with the parameters of the ESR spectra of $C_3H_6^{\cdot+}$ **17**, the data for both the $C_5H_8^{\cdot+}$ RC **3** and **4** and the $^{\cdot}CH_2Me$ radical **13** are given in Table 7.

Table 7 indicates that invoking the evaluated geometry (see Table 6) for RC **17** and **18** ensures good agreement between the experimental and AMNDO-UHF-calculated a^Z_{iso} constants (Z = ^1H and ^{13}C). The apparently excessive difference between the calculated and experimental result in the case of the C(β)(2) nucleus is explained by the fact that in the ethyl radical $^{\cdot}C(\alpha)H_2C(\beta)H_3$ and in RC **17**, **18** ($^{\cdot}C(\alpha)H_2C(\beta)H_2{}^+C(\gamma)H_2$), the structural-chemical environments of the C(β) atom are considerably different. When the geometry of RC **17** and **18** predicted *ab initio*[10] was used, all of the a^Z_{iso} IHFC constants calculated in the framework of AMNDO-UHF were equally satisfactory, except one ($a^{H(\beta)}_{iso}$), which was lower in magnitude than the experimental value by a factor of

Table 7. The AMNDO-UHF calculated IHFC constants (Oe) with ^1H and ^{13}C nuclei in $C_3H_6^{\cdot+}$ ($C_5H_8^{\cdot+}$) distonic RC

Nucleus[a]	*dist*(90.0)-$C_3H_6^{\cdot+}$ (**17**)			*dist*(0.90)-$C_3H_6^{\cdot+}$ (**18**)		
	experiment	geometry		experiment	geometry	
		ab initio	evaluation		*ab initio*	evaluation
H(1), H(2')	−22.7[b] (−22.7)[c]	−21.9	−22.1	—	−0.7	−0.8
H(2), H(2')(β)	30.2 (30.4)	15.4	30.0	− (14.7)[d]	10.0	13.2
H(3), H(3')	—	0.6	0.1	− (−21.6)	−22.2	−22.9
C(1)	− (39.1)[e]	38.1	37.0	—	5.5	7.9
C(2)(β)	− (−13.6)	−4.1	−5.0	− (−13.6)[e]	−5.5	−5.7
C(3)	—	−0.2	0.3	− (39.1)	36.4	36.1

[a] See Scheme 8 and Table 6. [b] 108 K, Freon-113, 1.0 mol. % of cyclopropane.[86] [c] **4**, 113 K, Freon-113, 1.0 mol. % VCP.[4] [d] **3**, 110 K, Freon-113, 0.01 mol. % VCP (this work). [e] for ^{13}C in $^{\cdot}CH_2CH_3$ (**13**), see Table 3.

almost two in the case of RC **17** and lower by one-third in the case of RC **18**.

These great deviations of the theoretical values of $a^{H(\beta)}_{iso}$ from the experimental values are undoubtedly caused by large errors in the *ab initio* calculations[10] performed for distonic RC **17** and **18**. This is indicated, in particular, by the correlation of the degree of the observed (see Table 7, Scheme 8) deviation (~15 and 5 Oe) of the isotropic constant with the non-coincidence (0.125 and 0.056 Å) between the empirically evaluated and *ab initio*[10] calculated lengths of the C(α)—C(β) bond corresponding to it. The inadequacy of the geometric parameters of RC **17** and **18** determined by the nonempirical UHF/6-31 G** method is most of all due to the known tendency of the UHF approximation to overestimate the stability of structures with unjustified low symmetry[10] and unusually extended C—C bonds.[8,30,33,87]

Thus, the results of the quantum-chemical analysis carried out (see Tables 5—7) indicate that the C(1)—C(2) and C(2)—C(3) bond lengths in type **17** and **18** distonic RC (see Schemes 8 and 9) differ slightly and are rather close to the values empirically evaluated by us (see Table 6) assuming a higher (C_{2v} instead of C_s) local symmetry of the C(β)(2)H_2 central group, and their equality. In spite of the obvious similarity of the spatial atomic configurations, the isoelectronic conformers **17** and **18** have rather dissimilar C(1)—C(2)—C(3) bond angles (90° and 116°, respectively). It is this angle that determines the specific electronic structure and reactivity of the distonic RC.

The stereoelectronic control of the thermal transformations of VCP$^{\cdot+}$

We studied the formation and subsequent thermal transformations of VCP$^{\cdot+}$ in X-irradiated frozen Freon matrices by ESR under conditions that correspond to the occurrence of radical reactions in both solid (Ref. 4) and gaseous (this work) VCP. It was found that, depending on the physical state, either *anti*-VCP$^{\cdot+}$ (in the solid VCP) or *gauche*-VCP$^{\cdot+}$ (in gaseous VCP) is produced. The direction of the subsequent selective cleavage of the cyclopropane ring (reactions (2*) and (6*)) resulting in the formation of one of the distonic RC (*dist*(90.0)- or *dist*(0.90)-$C_5H_8^{\cdot+}$) is determined, in turn, by the conformation of VCP$^{\cdot+}$. Specific electronic and geometric factors play a major role in these radical processes, which can be seen with the aid of quantum-chemical analysis that takes into account radiospectroscopic data.

Primary VCP$^{\cdot+}$. The chemical properties of a primary RC are determined to a large extent by its SOMO, which is mostly formed from the HOMO of the original molecule after removal of an electron from it. It is convenient to treat VCP as an organic compound of the type R—R′ built of cyclopropyl (R = *cyclo*-C_3H_5) and vinyl (R′ = $CHCH_2$) moieties. The correlation diagram of the interaction between the HOMO of these moieties is shown in Fig. 4. Since these HOMO have similar orbital energies, they interact rather strongly, which is manifested as a considerable decrease in the first ionization potential in the formation of the collective system (9.2 eV[22] for VCP compared to 10.6 eV[22] and 10.5 eV[78] for cyclopropane and ethylene, respectively). The (e_A—π) HOMO of VCP is characterized by π-type symmetry and is built predominantly of two p-AO of the vinyl group C atoms and one AO of the adjacent cyclopropyl C atom.

As can be seen from Fig. 4, the interaction of the VCP moieties removes the double degeneracy of the HOMO of the cyclopropane ring and is accompanied by its structural distortion. Using gas electron diffraction[9] in combination with the X-ray diffraction data and *ab initio* calculations, it has been found that in VCP, the cyclopropyl C—C bonds adjacent to the vinyl substituent are 0.015 Å longer and the C—C bond opposite the vinyl substituent is 0.010 Å shorter than the corresponding bonds in cyclopropane (D_{3h}, R(C—C) = 1.510 Å).[88] The *anti*-conformation of VCP, in which the plane of the vinyl fragment bisects the cyclopropane ring, is the most energetically favorable. At this orientation, the

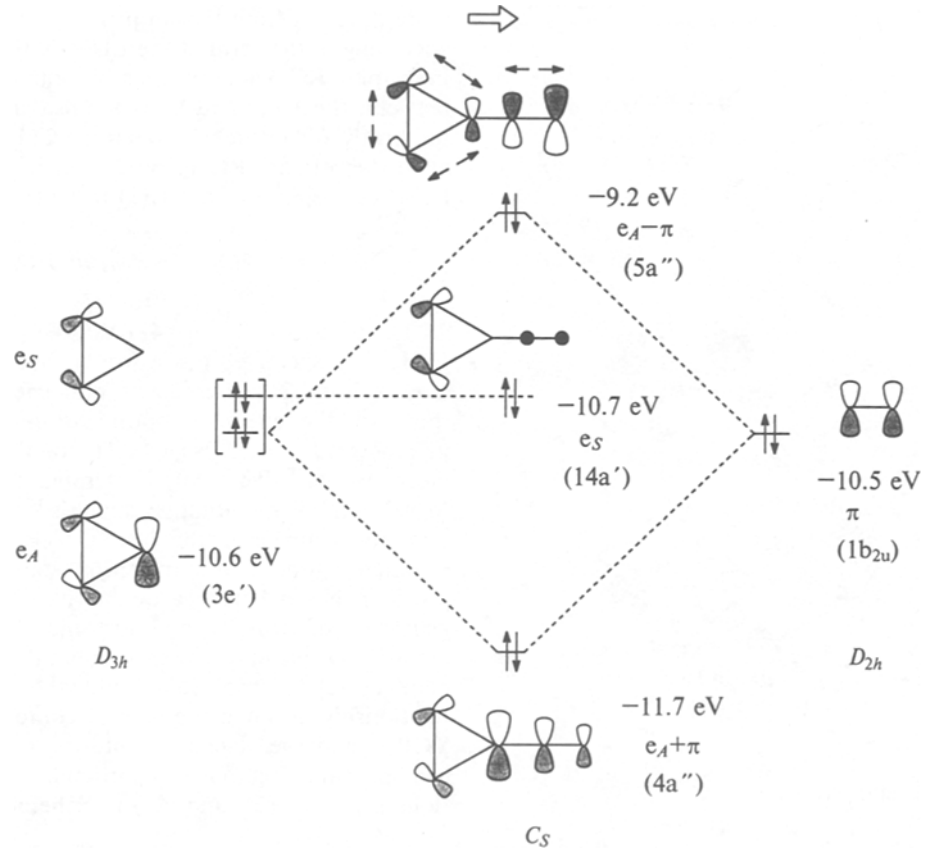

Fig. 4. The correlation diagram of the interaction between the MO of the VCP moieties and their structural distortions. The energies of MO have been evaluated (using Coupmans theorem) from the photoelectron spectra.[22,78] The large arrow denotes the direction of the partial electron transfer between the VCP moieties, and the paired arrows show the type of variation of the length (strength) of the C—C bond.[89]

π-MO of the vinyl group interacts with the antisymmetrical $3e'_A$-MO of the cyclopropane ring, and its structural distortion (see Fig. 4) indicates that this group has a π-acceptor character[89] and, therefore, its p-AO predominates in the (e_A—π) HOMO of VCP.

According to ESR and AMNDO-UHF data, the spin density in primary $VCP^{\cdot+}$ is almost completely localized at the vinyl substituent, which corresponds to ionization of the (e_A—π) HOMO of VCP. The comparative calculations of the geometric parameters of VCP and its RC in *anti*-conformations carried out by us (Fig. 5) make it possible to judge the structural distortions that accompany the single adiabatic ionization of the molecule more definitely. The $^2A''$ state of *anti*-$VCP^{\cdot+}$ detected by ESR is its ground state wherein the vinyl group is an even stronger π-acceptor, since it has a positive charge. The C(1)—C(3) and C(2)—C(3) bonds adjacent to it are lengthened by 0.065 Å (1.602—1.518), and the opposite C(2)—C(3) bond is shortened by 0.136 Å (1.382—1.518), while the $C(1)H—C(4)H=C(5)H_2$ moiety becomes geometrically similar to an allylic system.

According to calculations, the $^2A''$ state of *anti*-$VCP^{\cdot+}$ is 23.8 kcal mol^{-1} (1.03 eV) more stable than the alternative $^2A'$ state, which corresponds to the ionization of the occupied MO localized at the cyclopropane ring. Particular attention is attracted by the fact that the corresponding structural parameters of the excited *anti*-$VCP^{\cdot+}$ ($^2A'$) are identical to those of the unsubstituted cyclopropane RC[28,69] for which $^2A'$ is the ground state. The attempts to detect the excited *anti*-$VCP^{\cdot+}$ ($^2A'$) were unsuccessful, which is in good agreement with the great difference between the energies of the $^2A''$ and $^2A'$ states evaluated by MNDO (see Fig. 5).

The isomeric *gauche*-$VCP^{\cdot+}$ has a lower symmetry (C_1) than *anti*-$VCP^{\cdot+}$ (C_s). Thus, the cyclopropyl C—C bonds adjacent to the ionized vinyl substituent are nonequivalent, and, hence, the probabilities of their cleavage are different, due to their different strengths (lengths). The dihedral angles that characterize the arrangement of the C(1)—C(2) and C(1)—C(3) bonds with respect to the p_p-AO axis of the vinyl group in *gauche*-$VCP^{\cdot+}$ are 0° and 50—60°, respectively (*cf.* Fig. 5, Schemes 7 and 9, and Table 4). The C(1)—C(3)

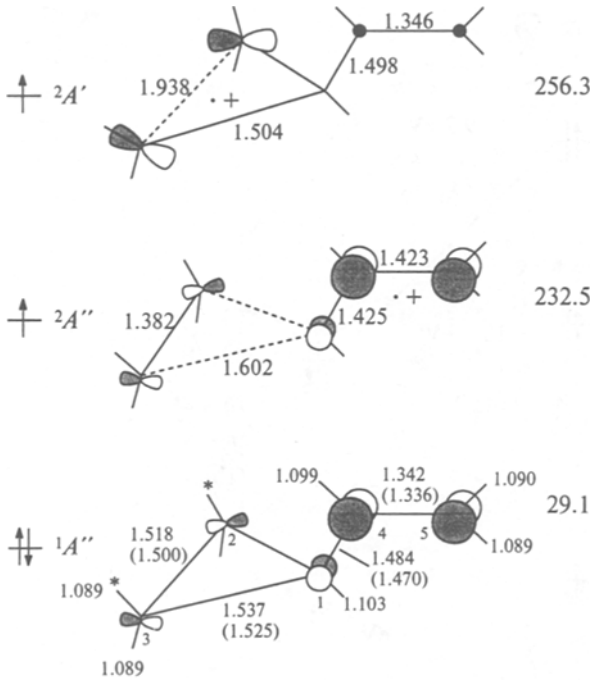

Fig. 5. The MNDO-UHF calculated structures and heats of formation of *anti*-VCP and two states ($^2A''$ and $^2A'$) of *anti*-VCP$^{\cdot+}$ corresponding to the similar symmetry of the two highest occupied MO of *anti*-VCP. The C—C and C—H (A) bond lengths from the gas electron diffraction data[9] are given in parentheses.

bond in this conformer participates much more efficiently in the direct delocalization of the spin density and the positive charge than the C(1)—C(2) bond, since it is more strongly conjugated with the π-system of the electron-deficient vinyl substituent. The same conclusion may in essence be drawn from the results of radiospectroscopic studies of the chemically induced dynamic nuclear polarization in the *gauche*-VCP$^{\cdot+}$ moiety incorporated in a series of bicyclic compounds.[90]

Judging from the character of both the HOMO in VCP and the SOMO in VCP$^{\cdot+}$ ($^2A''$), it would be expected that the partial electron transfer from the cyclopropane ring to the vinyl group would result in the selective weakening (lengthening) of the C(1)—C(3) bond in *gauche*-VCP$^{\cdot+}$. In fact, *ab initio* (STO-3G) calculations[91] indicate that the C(1)—C(3) bond in *gauche*-VCP$^{\cdot+}$ is somewhat longer (~1.57 Å) than the C(1)—C(2) bond (~1.54 Å).

Considering the foregoing, it seems quite reasonable that it is cleavage of the C(1)—C(3) bond of the cyclopropane ring in *gauche*-VCP$^{\cdot+}$ that we detected by ESR (see Scheme 9). The unpaired electron in the resulting distonic forms of $C_5H_8^{\cdot+}$ is distributed in a manner quite different from that in primary VCP$^{\cdot+}$ In addition, according to the form of the LUMO, the positive charge in distonic RC **3** and **4** is mostly about evenly distributed between the C(1) and C(5) atoms, rather than almost uniformly and entirely between the C(4) and C(5) atoms, as in the primary RC **1** and **2**, *i.e.*, the electron density has been displaced from C(1) to C(4).

Dist(0.90)- and dist(90.0)-$C_5H_8^{\cdot+}$

Distonic RC **3** and **4** (*dist*(0.90)- and *dist*(90.0)-$C_5H_8^{\cdot+}$, respectively) as a whole, like their cyclic precursors **1** and **2**, possess low symmetries (C_1 and C_S). In this case the energetic optimization of the structural parameters by the MNDO-UHF method may result in great errors.[28] Therefore, attempts to carry out the MNDO-UHF quantitative analysis of radical transformations occurring in the case of $C_5H_8^{+\cdot}$ *via* only low-symmetry ground and transition states can hardly be justified. Nevertheless, a qualitative comparison of the geometry of primary and distonic VCP$^{\cdot+}$, evaluated empirically using ESR spectra and certain structural data for related molecules, allows one to identify the relationship between the type of conformation of cyclic VCP$^{\cdot+}$ and the selective route of the cleavage of the cyclopropane ring to give a particular RC $C_5H_8^{\cdot+}$ (reactions (2), (2′), (6), and (6′) in Schemes 2, 5, and 10).

Scheme 10

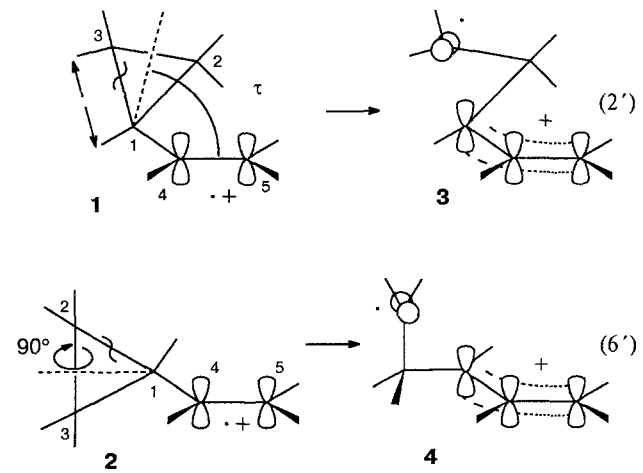

The primary *gauche*- and *anti*-VCP$^{\cdot+}$ belong to the class of energetically easily interconverting conformers, while the corresponding distonic RC **3** and **4** probably fall in the category of rather stable structural isomers with substantially different spatial and electronic structures. These distonic RC form (Scheme 10) and decay in independent processes in different physical states of the material, without direct interconversion by internal

rotation. However, despite the structural distinctions in the starting reactants and final products, the two contrasting thermal rearrangements of RC **1** and **2** exhibit the same specific character.

As can be seen from Scheme 10, the cleavage of the cyclopropane ring in both RC occurs, conventionally speaking, *via* a "single" rotation, *i.e.*, one of the terminal groups (either $^{\cdot}CH_2$ or $CHCHCH_2^+$) retains its spatial arrangement, while the other group rotates through 90°. Consequently, an allylic cationic system is formed in the distonic $C_5H_8^{\cdot+}$ structure from the vinyl carbon atoms and the next cyclopropyl carbon atom of the primary $VCP^{\cdot+}$, and the original mutual arrangement of the p-AO of these atoms is retained. In the thermal rearrangement of *gauche*-$VCP^{\cdot+}$ (reaction (2′)), the vinyl substituent fixes the neighboring p-AO that is across the cyclopropane ring, and in the rearrangement of *anti*-$VCP^{\cdot+}$ (reaction (6′)), the orbital along the cyclopropane ring is fixed, which is reflected by the designations *dist*(0.90) and *dist*(90.0), respectively.

All five of the C atoms in the *dist*(0.90)-$C_5H_8^{\cdot+}$ RC **3** are located in the same plane (see Scheme 10). The geometric parameters that change most significantly on going from *gauche*-$VCP^{\cdot+}$ to *dist*(0.90)-$C_5H_8^{\cdot+}$ are the length of the C(1)—C(3) bond being cleaved, the C(1)—C(2)—C(3) bond angle (from 60° to 116°), and also the dihedral angle τ (see Scheme 10), which is a measure of the difference in the spatial orientation of p_π-AO of the C(1), C(4), and C(5) atoms (for *gauche*-$VCP^{\cdot+}$, $\tau = 70°$). On the other hand, in the *dist*(90.0)-$C_5H_8^{\cdot+}$ RC **4**, only four C atoms lie in the same plane, while the fifth atom, corresponding to the terminal fragment, $^{\cdot}CH_2$, is located on the axis perpendicular to this plane. The thermal transformation of *anti*-$VCP^{\cdot+}$ into *dist*(90.0)-$C_5H_8^{\cdot+}$ is, most of all, the rotation of this fragment through 90° and the increase in the C(1)—C(2)—C(3) valence angle from 60° to 90°.

It is most likely that during the opening of the cyclopropane ring both terminal groups of the primary $VCP^{\cdot+}$ undergo concerted structural rearrangements. However, their combination is equivalent to the single-rotation mechanism of the formation of the distonic form of RC. One characteristic feature is that, unlike neutral molecules containing cyclopropane rings, the isostructural RC do not possess any elements of symmetry that are retained during the single-rotation rearrangement. In these cases, the generally applied quantum-chemical methods do not allow one to obtain reliable information on the mechanism of the RC rearrangements. Unfortunately, not very reliable quantum-chemical calculations of the pathways of the transformations of small radical systems (including the rearrangement of the cyclopropane RC to the propylene RC) have become rather widespread at present,[10,32,35,36,39–48,92] in spite of the apparent disagreement with experimental data.[8,30,33,49]

Taking into account the complexity of the problem and the insufficient capabilities of present-day quantum-chemical computer programs, it should not be expected that the attempts being presently undertaken to consider quantitatively the transition states in the structural rearrangements of low-symmetry RC will be successful. In this situation, the simple correlations and analogies that are extensively and efficiently used in the framework of the method of reactivity indices, which has shown itself to advantage, are of particular urgency.[93] First of all, it is necessary to search for the energetic and structural correlation between the ground states of neutral molecules and their RC guided by the principle of the subdivision of similar fragments into alternative sets depending on the degree of retention or change in their initial geometry.

In the context of this approach, the thermal rearrangement of VCP into cyclopentene occurring *via* a transition state having no elements of symmetry has been successfully described.[94] Using the terms suggested by us, this transition state has a structure of *dist*(90.60)-C_5H_8, since the migrating methylene group and the resulting allyl group rotate through 90° and 60°, respectively, relative to their original positions. The active bonding interaction that arises between these groups favors the isomerization of VCP into cyclopentene. The concept of the "single-rotation" mechanism of the cleavage of the cyclopropane ring in neutral molecules has been used recently for explaining characteristic features of *cis-trans* rearrangements.[95,96]

However, the primary RC formed initially in the ionization of VCP rearrange into relatively stable distonic forms in which the positive charge and the unpaired electron are completely separated due to the 90° rotation of only one of the terminal groups in $VCP^{\cdot+}$. Therefore, it cannot be ruled out that the fact that the ionized VCP, *i.e.*, VCP^+,[13] unlike the VCP itself,[97,98] does not isomerize into the cyclopentene structure in gas[99] or in the condensed phase[4,100] is caused by the "single-rotation" character of this rearrangement. Non-empirical quantitative calculations of the potential energy surfaces corresponding to all of the possible transformations of primary cyclic conformers **1** and **2**, the corresponding distonic isomers **3** and **4**, and also their low-symmetry cyclopentene and diene analogs would make it possible to judge this more definitely and with confidence. However, these non-empirical quantum-chemical calculations are now virtually impracticable, and it is unreasonable to hope that they will be carried out in the immediate future.

In view of the foregoing, it appears that the profiles of the potential energy surfaces of $C_6H_{10}^{\cdot+}$, including the RC of vinylcyclobutane and cyclohexene, along with the distonic forms, like RC **3** and **4**, which have been recently[101] calculated *ab initio*, deserve a separate thorough examination. Unfortunately, structural rearrangements of the vinylcyclobutane RC have not yet been studied by ESR, and the theoretical evaluations of the a^Z_{iso} IHFC constants (see Ref. 101), which would facilitate the quantum-chemical analysis, have not been car-

Scheme 11

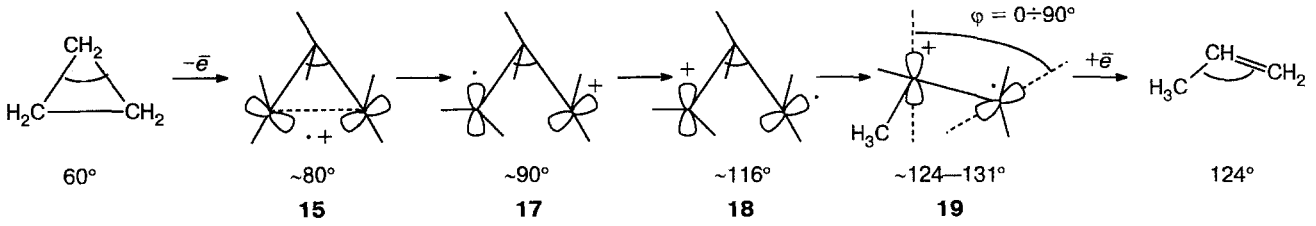

ried out. Therefore, it is difficult to judge the adequacy of the *ab initio* calculated geometric parameters of the four RC listed and the structural-chemical conclusions based on these results. Nevertheless, the qualitative reasoning previously proposed[101] for $C_6H_{10}^{\cdot+}$ is in agreement with the data presented by us for $C_5H_8^{\cdot+}$ concerning the stereoelectronic structure of the intermediate distonic forms, which does not allow their subsequent transformation into cycloalkene RC.

On the other hand, the potential energy surface of $C_3H_6^{\cdot+}$,[10,35,36,45,58,92,102—104] which rejects the existence of distonic structures and was most thoroughly constructed by *ab initio* methods, is at variance with various experimental data.[6,14,78] However, in our opinion, these contradictions are eliminated rather easily, if one takes into account the above-analyzed analogy of $C_3H_6^{\cdot+}$ and $C_5H_8^{\cdot+}$ and considers the scheme of the gas-phase rearrangement of the cyclopropane RC (**15**) into the propylene RC (**19**) in which the C(1)—C(2)—C(3) bond angle acts as a reaction coordinate (Scheme (11)).

According to Scheme 11, ionization of the cyclopropane molecule results in an increase in the C(1)—C(2)—C(3) bond angle from 60° to 80° and then to 90°, and the cyclic $C_3H_6^{\cdot+}$ form is simultaneously transformed into the distonic form (RC **17**) by a "single rotation". As this angle increases further from 90° to 116°, RC **17** is converted into RC **18**, which has a qualitatively different electronic structure. At the next stage, the angle increases from 116° to 124—131°, which causes the 1,2-migration of a hydrogen atom to give propylene RC **19** with a twisted structure, and the greatest bond angle of 131° is matched by an angle of twist φ of 45°.[105]

In terms of this scheme, in agreement with experimental data,[8,33,105,106] it is twisted, rather than planar,[10,45] RC **19** that is formed, and prior to it, the 1,2-distonic RC **19**, for which φ = 90° and the C(1)—C(2)—C(3) bond angle is probably close to 120°, could have been produced during the 1,2-migration of the H atom. It cannot be ruled out that the φ angle in RC **19** depends substantially on the above-mentioned bond angle, since its magnitudes of 131° and 124° (calculated by various methods) are matched by φ = 45° and φ = 0 to 17° (see Refs. 10, 45, and 105). Notice that 1,2-distonic RC resulting from indirect ionization of trimethylsilylethylene[107] and octamethyl substituted bicyclopentylidene[108,109] have already been detected in frozen Freon matrices by ESR. The addition of an electron to RC **19** completes the rearrangement of cyclopropane into propylene with angles φ = 0° and C(1)—C(2)—C(3) = 124°.[110]

Conclusions

The recently developed technique of ESR spectroscopy in frozen Freon matrices allows an adequate simulation of the elementary steps of gas-phase thermal transformations of highly reactive hydrocarbon radical cations. For this purpose, rather dilute solutions of hydrocarbons in Freons in a limited temperature range (0.1—1.0 mol. % and 77—150 K for polycrystalline $CFCl_3$; 0.01—0.1 mol. % and 77—110 K for amorphous $CFCl_2CF_2Cl$) are used, and the specimens are frozen at 77 K and irradiated with X-rays in a dose of ~0.5 Mrad. The conditions of the experiment are practically identical for the majority of matrices used, since the properties of frozen Freons are rather close to those of either $CFCl_3$ or $CFCl_2CF_2Cl$. The observance of the above-specified conditions, first, prevents the RC formed from contacting the unchanged molecules of the original hydrocarbon owing to their low concentration in the rigid matrix and, second, minimizes the effect of the matrix environment on the geometric and electronic structures of RC.

When the concentration of a hydrocarbon is high (0.1—100 mol. %), the reactions of RC in the solid phase are simulated at the same temperatures, since more and more RC contain nonionized molecules in their environment. Nevertheless, on going from the "gas-phase" to "solid" conditions (from 0.01 to 1.0 mol. %) in amorphous $CFCl_2CF_2Cl$, the absolute (total) number of structurally isolated regions corresponding to the gas-phase stabilized RC is retained, in spite of the obvious changes in the matrix environment. However, the relative proportion of these regions ultimately becomes 100-fold lower than that of the "solid" regions.

Well-resolved ESR spectra of RC when the hydrocarbon concentration in the $CFCl_2CF_2Cl$ matrix is 0.01 mol. % are only recorded in a rather narrow temperature range, 100—110 K. Below 100 K and above 110 K, the ESR signals of the matrix radicals predominate. In addition, rather stringent requirements are im-

posed upon the dose of irradiation. In more concentrated (≥1.0 mol. %) solutions, the dependence of the ESR spectra on the irradiation dose is less pronounced, and above 110 K ion-molecular reactions typical of the condensed phase occur. RC existing under the "gas-phase" conditions exhibit narrower ESR lines (ΔH = 3 to 6 Oe) than those in a solid (ΔH = 6 to 10 Oe).

The amount of structural information in the ESR spectra increases dramatically when an adequate quantum-chemical method is used for the interpretation. However, the most common standard semiempirical versions of NDO-UHF (INDO, MNDO, AM1, and others) are in many cases unsuitable for obtaining reliable structural data from the ESR spectra of hydrocarbon RC. The most appropriate method for this purpose is the adapted version of MNDO (AMNDO-UHF), which is characterized, first, by the presence of two theoretically justified coefficients of proportionality, $K(H(\alpha))$ = 415 Oe and $K(H(\beta))$ = 850 Oe, between the spin densities $\rho_s^{H(\alpha)} < 0$ and $\rho_s^{H(\beta)} > 0$, respectively, and the $a^H_{iso} = K(H)\rho_s^H$ constants of IHFC with protons (for carbon nuclei, $K(C)$ = 650 Oe) and, second, by the preliminary fragment-for-fragment construction of the geometry of the hydrocarbon RC. This can be done using the unified dependences between the geometric and electronic structures of the same fragments incorporated in well-known molecules and free radicals.

The results of quantum-chemical analysis in combination with ESR data indicate that VCP and its radical-cation form, $VCP^{\cdot +}$, are rather convenient objects that allow detailed investigation of the peculiarities of the aggregate state of a substance. VCP possesses lower structural rigidity than the hydrocarbon compounds that have been previously studied in this respect. In particular, internal rotation about the C—C bond between the cyclopropyl and vinyl molecular moieties occurs without substantial obstacles. Owing to this, the *gauche*-VCP/*anti*-VCP ratio is sensitive to phase transformations of the material, though in the molecule *anti*-conformation predominates in all cases. The ratio between the primary radical-cation forms, $VCP^{\cdot +}$, resulting from ionization is much more sensitive to the aggregate state of the medium: *gauche*-$VCP^{\cdot +}$ is more stable in the gas phase, and *anti*-$VCP^{\cdot +}$ is more stable in the condensed phase.

The positive charge in the primary $VCP^{\cdot +}$ conformers formed by irradiation is mostly concentrated at the vinyl group, and the neighboring C—C bonds of the cyclopropane ring are substantially lengthened (*i.e.*, weakened), while the opposite C—C bond is shortened (*i.e.*, strengthened). Due to the cleavage of one of the weakened C—C bonds, which is accompanied by displacement of an electron to the π-accepting vinyl substituent, *anti*-$VCP^{\cdot +}$ is converted into the thermodynamically less favorable distonic RC, *dist*(90.0)-$C_5H_8^{\cdot +}$, in the condensed phase, and *gauche*-$VCP^{\cdot +}$ is converted into the more favorable *dist*(0.90)-$C_5H_8^{\cdot +}$ in the gas phase. The C(α)—C(β)—C(γ) bond angles in these distonic RC are ~90° and ~116°, respectively (rather than ~60° as in the original cyclopropane ring). It is mostly this angle that determines the specific features of the electronic structure and reactivity of the distonic RC.

In particular, the mechanism of the gas-phase rearrangement of the cyclopropane RC to the propylene RC assuming the intermediate participation of the corresponding distonic radical cations, may be related to the increase in this angle from 60° to ~120° (see Scheme 11). At the same time, it should be noted that, because of the specific character of the analogous monomolecular rearrangement of primary $VCP^{\cdot +}$ into the distonic structures combined with the rather high stability of the latter, $VCP^{\cdot +}$ does not undergo thermal isomerization into the cyclopentene form, though VCP itself readily undergoes this transformation both in the gas and condensed phases.

The direction of thermal transformations of hydrocarbon RC in frozen Freon matrices depends on the state of the medium. For example, under the conditions that simulate a rarefied gas, *anti*-$VCP^{\cdot +}$ undergoes monomolecular isomerization into the more stable conformer, *gauche*-$VCP^{\cdot +}$, which is then converted into the *dist*(0.90)-$C_5H_8^{\cdot +}$ distonic RC. At a somewhat higher concentration of VCP, the "σ-dimeric" distonic RC, $^{\cdot}CH_2CH_2CHCH(CH_2)_3CHCHCH_2^{\cdot +}$, is produced due to the addition of *dist*(0.90)-$C_5H_8^{\cdot +}$ at the double bond of an *anti*-VCP molecule. In this case, *anti*-$VCP^{\cdot +}$ reacts with *anti*-VCP to give the *dist*(90.0)-$C_5H_8^{\cdot +}$ distonic structure, which is formed in the same way it is formed in the condensed phase.

This work was carried out with the financial support of the Russian Foundation for Basic Research (Project No. 93-03-04075).

References

1. D. Serep, I. D'erd', M. Roder, and L. Woinarovich, *Radiatsionnaya khimiya uglevodorodov* [*Radiation Chemistry of Hydrocarbons*], Ed G. Fel'diak, Energoatomizdat, Moscow, 1985, 304 p. (Russ. Transl.).
2. V. I. Fel'dman, F. F. Sukhov, and H. A. Slovokhotova, *Vysokomol. Soed., B*, 1994, **36**, 519 [*Polym. Sci. USSR*, 1994, **36** (Engl. Transl.)].
3. M. C. R. Symons, *Chem. Soc. Rev.*, 1984, **13**, 393.
4. I. Yu. Shchapin, V. I. Fel'dman, V. H. Belevskii, H. A. Donskaya, and N. D. Chuvylkin, *Izv. Akad. Nauk, Ser. Khim.*, 1994, 11 [*Russ. Chem. Bull.*, 1994, **43**, 1 (Engl. Transl.)].
5. I. A. Baranova, V. H. Belevskii, and V. I. Fel'dman, *Vestn. Mosk. Univ., Ser. 2 Khim.* [*Bull. Mosc. Univ., Div. 2, Chem.*], 1987, **28**, 137 (in Russian).
6. X.-Z. Qin and F. Williams, *Tetrahedron*, 1986, **42**, 6301.
7. T. Clark, A. Hasegawa, and M. C. R. Symons, *Chem. Phys. Lett.*, 1985, **116**, 79.
8. S. Lunell, L. A. Eriksson, and M.-B. Huang, *J. Mol. Struct. (Theochem.)*, 1991, **230**. 263.
9. M. Traetteberg, P. Bakken, A. Almennigen, and W. L'ttke, *J. Mol. Struct.*, 1988, **189**, 357.

10. P. Du, D. A. Hrovat, and W. T. Borden, *J. Am. Chem. Soc.*, 1988, **110**, 3405.
11. J. Fujisawa, T. Takayanaci, S. Sato, and K. Shimokoshi, *Bull. Chem. Soc. Jpn.*, 1988, **61**, 1527.
12. J. K. Kochi, P. J. Krusic, and D. R. Eaton, *J. Am. Chem. Soc.*, 1969, **91**, 1877, 1879.
13. I. Yu. Shchapin, V. I. Fel'dman, and V. H. Belevskii, *Dokl. Akad. Nauk*, 1994, **334**, 338 [*Dokl. Chem.*, 1994, **334** (Engl. Transl.)].
14. V. G. Zaikin, A. M. Mikaya, and V. M. Vdovin, *Mass-spektpometpiya malykh tsiklov (C, Si, Ge)* [*Mass Spectrometry of Small Cycles (C, Si, Ge)*], Nauka, Moscow, 1983, 160 p. (in Russian).
15. L. B. Knight, Jr., *Acc. Chem. Res.*, 1986, **19**, 313.
16. J. L. Courtneidge and A. G. Davies, *Acc. Chem. Res.*, 1987, **20**, 90.
17. D. W. Werst, M. G. Bakker, and A. D. Trifunac, *J. Am. Chem. Soc.*, 1990, **112**, 40.
18. Z. V. Todpes, *Elektronnyi perenos v organicheskoi i metalloorganicheskoi khimii, Ser. organich. khimiya* [*Electron Trasnsfer in Organic and Organometallic Chemistry, the Organic Chemistry Series*], VINITI, Moscow, 1989, **12** (in Russian).
19. F. Gerson, *Acc. Chem. Res.*, 1994, **27**, 63.
20. W. Tang and T. Bally, *J. Phys. Chem.*, 1993, **97**, 4365.
21. W. Tang, X.-L. Zhang, and T. Bally, *J. Phys. Chem.*, 1993, **97**, 4373.
22. R. Gleiter, *Top. Curr. Chem.*, 1979, **86**, 197.
23. V. H. Belevskii, S. I. Belopushkin, and V. I. Fel'dman, *Dokl. Akad. Nauk SSSR*, 1990, **310**, 897 [*Dokl. Chem.*, 1990, **310** (Engl. Transl.)].
24. J. Westerling and A. Lund, *Chem. Phys.*, 1990, **140**, 421.
25. K. Toriyama, M. Okazaki, and K. Nunome, *J. Chem. Phys.*, 1991, **95**, 3955.
26. X.-Z. Qin and A. D. Trifunac, *J. Phys. Chem.*, 1991, **95**, 6466.
27. Yu. V. Rakitin, G. M. Larin, and V. V. Mikaya, *Interpretatsiya spektrov EPR koordinatsionnykh soedinenii* [*Interpretation of ESR spectra of Organic Compounds*], Nauka, Moscow, 1993, 339 p. (in Russian).
28. N. D. Chuvylkin, I. Yu. Shchapin, V. L. Klochikhin, V. A. Tikhomirov, and V. I. Fel'dman, *Vestn. Mosk. Univ., Ser. 2, Khim.* [*Bull. Mosc. Univ., Div. 2. Chem.*], 1992, **33**, 307 (in Russian).
29. G. I. Zhidomirov, P. V. Schastnev, and N. D. Chuvylkin, *Kvantovo-khimicheskie raschety magnitno-rezonansnykh parametrov* [*Quantum-Chemical Calculations of Magnetic Resonance Parameters*], Nauka, Novosibirsk, 1978, 368 p. (in Russian).
30. M.-B. Huang and S. Lunell, *Chem. Phys.*, 1990, **147**, 85.
31. S. Lunell, D. Feller, and E. R. Davidson, *Theor. Chim. Acta*, 1990, **77**, 111.
32. S. Lunell, L. A. Eriksson, and L. Worstbrock, *J. Am. Chem. Soc.*, 1991, **113**, 7508.
33. L. A. Eriksson, S. Lunell, and R. J. Boyd, *J. Am. Chem. Soc.*, 1993, **115**, 6896.
34. S. Lunell, L. A. Erikson, T. Fängström, J. Maruani, L. Sjöqist, and A. Lund, *Chem. Phys.*, 1993, **171**, 119.
35. D. D. M. Wayner, R. J. Boyd, and D. R. Arnold, *Can. J. Chem.*, 1983, **61**, 2310.
36. D. D. M. Wayner, R. J. Boyd, and D. R. Arnold, *Can. J. Chem.*, 1985, **63**, 3283.
37. T. Clark and S. F. Nelsen, *J. Am. Chem. Soc.*, 1988, **110**, 868.
38. K. Toriyama, R. Nunome, and M. Iwasaki, *J. Chem. Phys.*, 1982, **77**, 5891.
39. D. J. Bellville, R. Chelsky, and N. L. Bauld, *J. Comput. Chem.*, 1982, **3**, 548.
40. N. L. Bauld, D. J. Bellville, P. Pabon, R. Chelsky, and G. Green, *J. Am. Chem. Soc.*, 1983, **105**, 2378.
41. M. J. S. Dewar and K. M. Merz, Jr., *J. Mol. Struct. (Theochem.)*, 1985, **122**, 59.
42. J. N. Younathan and M. A. Fox, *J. Mol. Struct. (Theochem.)*, 1988, **163**, 163.
43. J. N. Aebischer, T. Bally, K. Roth, E. Haselbach, F. Gerson, and X.-Z. Qin, *J. Am. Chem. Soc.*, 1989, **111**, 7909.
44. S. Lunell, L. A. Eriksson, T. Fängstöm, J. Maruani, L. Sjöqvist, and A. Lund, *Chem. Phys.*, 1993, **171**, 119.
45. T. Clark, *J. Am. Chem. Soc.*, 1987, **109**, 6838.
46. N. L. Bauld, *J. Am. Chem. Soc.*, 1992, **114**, 5800.
47. P. Jungwirth, P. Cársky, and T. Bally, *J. Am. Chem. Soc.*, 1993, **115**, 5776.
48. P. Jungwirth and T. Bally, *J. Am. Chem. Soc.*, 1993, **115**, 5783.
49. M. Iwasaki, K. Toriyama, and K. Nunome, *Faraday Discuss. Chem. Soc.*, 1984, **78**, 19.
50. P. Bishof and G. Friedrich, *J. Comput. Chem.*, 1982, **3**, 486.
51. M. J. S. Dewar and W. Thiel, *J. Am. Chem. Soc.*, 1977, **99**, 4899.
52. D. M. Chipman, *J. Chem. Phys.*, 1979, **71**, 761.
53. L. B. Knight, Jr., J. M. Winiski, P. Miller, C. A. Arrington, and D. Feller, *J. Chem. Phys.*, 1989, **91**, 4468.
54. D. Feller and E. R. Davidson, *J. Chem. Phys.*, 1984, **80**, 1006.
55. T. A. Claxton, T. Chen, M. S. R. Symons, and G. Glidewell, *Faraday Discuss. Chem. Soc.*, 1984, **78**, 121.
56. D. Feller and E. R. Davidson, *Theor. Chem. Acta.*, 1985, **68**, 57.
57. S. Lunell and M.-B. Huang, *J. Chem. Soc. Chem. Commun.*, 1989, 1031.
58. W. J. Bouma, D. Poppinger, and L. Radom, *Isr. J. Chem.*, 1983, **23**, 21.
59. G. M. Zhidomirov and N. D. Chuvylkin, *Theoret. Chim. Acta (Berl.)*, 1973, **30**, 197.
60. M. N. Paddon-Row, D. F. Fox, J. A. Pople, K. N. Houk, and D. W. Pratt, *J. Am. Chem. Soc.*, 1985, **107**, 7696.
61. C. Glidewell, *J. Chem. Soc., Perkin Trans. 2*, 1983, **8**, 1285.
62. S. F. Nelsen, *J. Chem. Soc., Perkin Trans. 2*, 1988, **6**, 1005.
63. P. Bischof, *J. Am. Chem. Soc.*, 1976, **98**, 6844.
64. A. T. Amos and L. C. Snyder, *J. Chem. Phys.*, 1964, **41**, 1773.
65. D. M. Camaioni, *J. Am. Chem. Soc.*, 1990, **112**, 9475.
66. N. J. Hehre, L. Radom, P. R. Schleyer, and J. Pople, *Ab initio Molecular Orbital Theory*, WIP, New York, 1986.
67. C. Glidewell, *J. Chem. Soc., Perkin Trans. 2*, 1984, **3**, 407.
68. K. B. Wiberg, R. F. W. Bader, and C. D. Lau, *J. Am. Chem. Soc.*, 1987, **109**, 985.
69. O. Bastiansen, F. N. Fritsch, and K. Hedberg, *Acta Crystallogr.*, 1964, **17**, 538.
70. K. Kuchitsu, *J. Am. Chem. Soc.*, 1968, **49**, 4456.
71. M. Guerra, *J. Am. Chem. Soc.*, 1992, **114**, 2077.
72. P. J. Krusic, P. Meakin, and J. P. Jesson, *J. Phys. Chem.*, 1971, **75**, 3438.
73. V. S. Mastryukov and E. L. Osina, *J. Mol. Struct.*, 1977, **36**, 127.

74. L. V. Vilkov, I. S. Mastryukov, and N. I. Sadova, *Opredelenie geometricheskogo stroeniya svobodnykh molekul* [*Determination of the Geometric Structures of Free Molecules*], Khimiya, Leningrad, 1978, 224 p (in Russian).
75. O. V. Dorofeeva, V. S. Mastryukov, N. L. Allinger, and A. Almenningen, *J. Phys. Chem.*, 1990, **94**, 8044.
76. V. S. Mastryukov and I. Yu. Shchapin, *Vestn. Mosk. Univ., Sep. 2, Khim.* [*Bull. Mosc. Univ., Div. 2, Chem.*], 1991, **32**, 569 (in Russian).
77. I. Yu. Shchapin and V. S. Mastryukov, *J. Mol. Struct.*, 1992, **268**, 307.
78. I. F. Traven', *Elektronnaya struktura i svoistva organicheskikh molekul* [*The Electronic Structures and Properties of Organic Molecules*], Khimiya, Moscow, 1989, 384 p. (in Russian).
79. *Application of Electronic Structure Theory*, Ed. H. F. Schaefer III, Plenum Press, 1977, 357.
80. K. Kimura, S. Katsumata, and Y. Achiba, *Handbook of HeI Photoelectron Spectra of Fundamental Organic Molecules*, Japan Sci. Soc. Press, Tokyo, 1981, 266 p.
81. T. Egawa, T. Fukuyama, S. Yamamoto, F. Takabayashi, H. Kambara, T. Ueda, and K. Kuchitsu, *J. Chem. Phys.*, 1987, **86**, 6018.
82. W. J. Adams, H. J. Geise, and L. S. Bartell, *J. Am. Chem. Soc.*, 1970, **92**, 5013.
83. R. L. Hilderbrandt, J. D. Wieser, and L. K. Montgomery, *J. Am. Chem. Soc.*, 1973, **95**, 8598.
84. *Molecular Structure by Diffraction Methods*, Eds. G. A. Sim and L. E. Suttion, Chem. Soc., London, 1973, **1**, 824 p.; 1974, **2**, 513 p.; 1975, **3**, 514 p.
85. S. Yamamoto, M. Nakata, T. Fukuyama, and K. Kuchitsu, *J. Phys. Chem.*,1985, **89**, 3298.
86. X.-Z. Qin and F. Williams, *Chem. Phys. Lett.*, 1984, **112**, 79.
87. B. E. Watkins, J. S. Kiely, and H. Rapoport, *J. Am. Chem. Soc.*, 1982, **104**, 5702.
88. A. I. Ioffe, V. A. Svyatkin, and O. M. Nefedov, *Stroenie proizvodnykh tsiklopropana* [*Structures of Cyclopropane Derivatives*], Nauka, Moscow, 1986, 160 p.(in Russian).
89. R. R. Kostikov and A. F. Khlebnikov, *Sovremennye problemy organicheskoi khimii* [*The Present-day Problems of Organic Chemistry*], 1982, **7**, 36 (in Russian).
90. H. D. Roth and T. Herbertz, *J. Am. Chem. Soc.*, 1993, **115**, 9804.
91. L. T. Scott, I. Erden, W. R. Brunsvold, T. H. Schultz, K. N. Houk, and M. N. Paddon-Row, *J. Am. Chem. Soc.*, 1982, **104**, 3659.
92. C. E. Hudson, C. S. Giam, and D. J. McAdoo, *J. Org. Chem.*, 1993, **58**, 2017.
93. N. D. Chuvylkin and G. M. Zhidomipov, *Kvantovaya khimiya i organicheskii kataliz, Sep. kinetika i kataliz,* [*Quantum Chemistry and Organic Catalysis, the Kinetics and Catalysis series*], VINITI, Moscow, 1980, **8** (in Russian).
94. J. J. Quirante, F. Enriquez, and J. M. Hernando, *J. Mol. Struct. (Theochem.)*, 1990, **204**, 193.
95. Y. Yamaguchi, H. F. Schaefer III, and J. E. Baldwin, *Chem. Phys. Lett.*, 1991, **185**, 143.
96. S. J. Getty, E. R. Davidson, and W. T. Borden, *J. Am. Chem. Soc.*, 1992, **114**, 2085.
97. T. Hudlicky, T. M. Kutchan, and S. M. Naqvi, *Organic Reactions*, 1985, **33**, 247.
98. Z. Goldsdchmit and B. Crammer, *Chem. Soc. Rev.*, 1988, **17**, 229.
99. C. Dass, D. A. Peake, and M. L. Gross, *J. Mass. Spectrom.*, 1986, **21**, 741.
100. J. P. Dinnosenzo and D. A. Conlon, *J. Am. Chem. Soc.*, 1988, **110**, 2324.
101. N. L. Bauld, *J. Comput. Chem.*, 1990, **11**, 896.
102. D. A. Hrovat, P. Du, and W. T. Borden, *Chem. Phys. Lett.*, 1986, **123**, 337.
103. K. Ohta, H. Nakatsuji, H. Kubodera, and T. Shida, *Chem. Phys.*, 1983, **76**, 271.
104. S. Lunell, M.-B. Huang, and A. Lund, *Faraday Discuss. Chem. Soc.*, 1984, **78**, 35.
105. M. Shiotani, Y. Nagata, and J. Sohma, *J. Phys. Chem.*, 1984, **88**, 4078.
106. R. Toriama, K. Nunome, and M. Iwasaki, *Chem. Phys. Lett.*, 1984, **107**, 86.
107. G. W. Eastiand, Y. Kurita, and M. C. R. Symons, *J. Chem. Soc., Perkin Trans. 2*, 1984, 1843.
108. F. Gerson, J. Lopez, A. Krebs, and W. Ruger, *Angew. Chem. Int. Ed. Engl.*, 1981, **20**, 95.
109. V. H. Eierdanz and A. Berndt, *Angew. Chem.*, 1982, **94**, 716.
110. I. Tokue, T. Fukuyama, and K. Kuchitsu, *J. Mol. Struct.*, 1973, **17**, 207.

Received October 21, 1994